Electronic Supplementary Material (ESI) for Organic & Biomolecular Chemistry.
This journal is © The Royal Society of Chemistry 2018

Electronic supplementary information

for

Photodeamination to quinone methides in cucurbit[n]urils: potential application in drug delivery

Đani Škalamera,[†] Marija Matković,[†] Lidija Uzelac,[‡] Marijeta Kralj,[‡] Kata Mlinarić-Majerski,[†] Cornelia Bohne,[§,#]* and Nikola Basarić[†]*

[†] Department of Organic Chemistry and Biochemistry, Ruđer Bošković Institute, Bijenička cesta 54, 10 000 Zagreb, Croatia. Fax: + 385 1 4680 195; Tel: +385 1 4561 141

[‡] Division of Molecular Medicine, Ruđer Bošković Institute, Bijenička cesta 54, 10 000 Zagreb, Croatia

[§] Department of Chemistry, University of Victoria, Box 1700 STN CSC, Victoria BC, V8W 2Y2, Canada.

[#] Centre for Advanced Materials and Related Technologies (CAMTEC), University of Victoria, Box 1700 STN CSC, Victoria BC, V8W 2Y2, Canada.

Corresponding authors' E-mail addresses: CB cornelia.bohne@gmail.com, NB nbasaric@irb.hr

Contents:

1. Structure of Cucurbit[n]urils

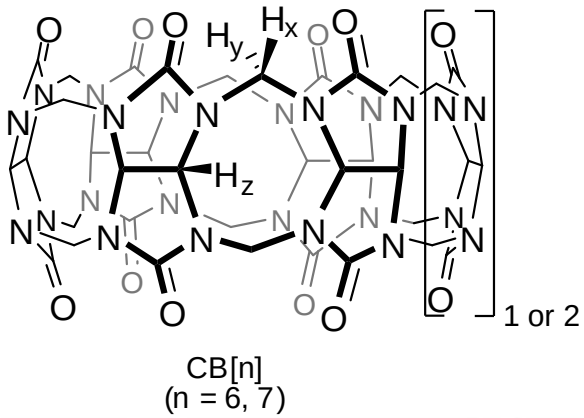

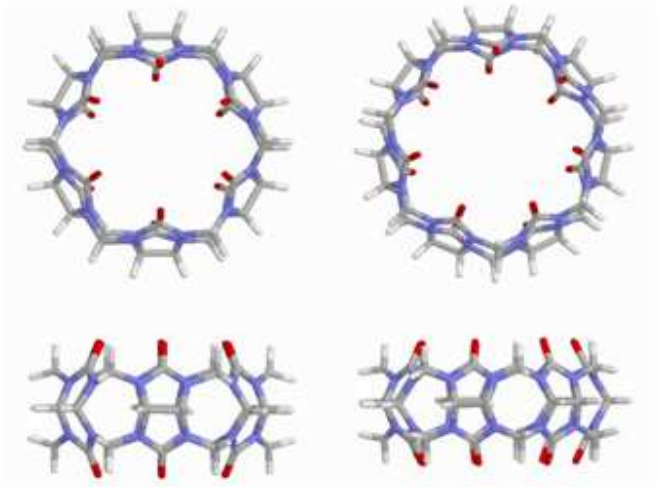

Fig S1. Structure of cucurbit[n]urils, CB[6] and CB[7].

2. Experimental section

General

^{1}H and ^{13}C NMR spectra were recorded at 300 or 600 MHz at 25 °C in D_2O using solvent residual peak as a reference (4.79 ppm). Chemical shifts were reported in ppm. Sodium deuteriophosphate buffers were prepared by mixing calculated amount of 85% D_3PO_4 in D_2O and 40% NaOD in D_2O (all chemicals were purchased from the usual commercial sources). pH value was measured for each buffer using electrode previously calibrated with two buffer solutions, pH 4.00 and pH 7.00. Sodium phosphates (p. a.) and acetonitrile (HPLC grade) were purchased from the usual commercial sources and were used as received. Water (H_2O) was purified by Mili-Q system. Irradiation experiments were performed in a reactor equipped with 8 lamps with the output at 300 nm (1 lamp 8W).

Preparation of the solution for UV-vis and LFP measurements

The following solutions were prepared:

1. A stock solution of **1** was prepared by dissolving 12.8 mg in 10 mL CH_3CN ($c = 6.35 \times 10^{-3}$ M).
2. A series of buffer solutions (c = 0.2 M) was prepared by dissolving appropriate quantity of NaH_2PO_4, Na_2HPO_4 or Na_3PO_4.
3. A stock solution of CB[6] was prepared by dissolving 94.5 mg of CB[6], and 146 mg of NaCl in 25 mL of deionized water (c (CB[6]) = 3.87×10^{-3} M, c (NaCl) = 0.100 M). To determine real concentration, titration was performed.[1] The CB[6] was 90.4% pure. The corrected concentration after titration was: 3.50×10^{-3} M.
4. Stock solution of CB[7] was prepared by dissolving 281.7 mg of CB[7], and 146 mg NaCl in 25 mL of deionized water (c (CB[7]) = 9.70×10^{-3} M, c (NaCl) = 0.100 M). To determine real concentration, titration was performed.[1] The CB[7] was 71% pure. The corrected concentration after titration was: 6.79×10^{-3} M.
5. A series of solutions at different pH was prepared by taking the CH_3CN solution of **1** (0.5 mL), appropriate sodium phosphate buffer (c = 0.2 M, 2.5 mL), and topping up to 5 mL with deionized water.

6. A series of solutions at different pH values was prepared, taking the CH_3CN solution of **1** (0.5 mL), the stock solution of CB[6] (0.5 mL or 2.0 mL), appropriate sodium phosphate buffer (*c* = 0.2 M, 2.5 mL), and topping up to 5 mL with deionized water (if needed).

7. A series of solutions at different pH was prepared taking the CH_3CN solution of **1** (0.5 mL), the stock solution of CB[7] (0.5 mL), appropriate sodium phosphate buffer (*c* = 0.2 M, 2.5 mL), and topping up to 5 mL with deionized water.

8. A stock solution of **2** was prepared by dissolving 16.0 mg in 10 mL CH_3CN (c = 5.42×10^{-3} M). Stock solution was prepared twice, a different stock was used for the measurement in the presence of CB[6].

9. The solutions of **2** were prepared by taking the stock CH_3CN solution of **2** (0.7 mL), appropriate sodium phosphate buffer (*c* = 0.2 M, 2.5 mL), and topping up to 5 mL with deionized water.

10. A series of solutions at different pH values was prepared, taking the CH_3CN solution of **2** (0.7 mL), the stock solution of CB[6] (2.0 mL), and topping up to 5 mL with the appropriate sodium phosphate buffer (*c* = 0.2 M, 2.5 mL).

11. A series of solutions at different pH values was prepared containing CB[7], taking the CH_3CN solution of **2** (0.7 mL), the stock solution of CB[7] (0.5 mL), and appropriate sodium phosphate buffer (*c* = 0.2 M, 2.5 mL), and topping up to 5 mL with deionized H_2O.

The concentration of **1** in all samples for the measurements was *c* = 6.35×10^{-4} M, concentration of sodium phosphate buffer was 0.1M, CB[6] was 3.50×10^{-4} M or 1.40×10^{-3} M, and CB[7] was 6.79×10^{-4} M.

The concentration of **2** in all samples for the measurements was *c* = 7.59×10^{-4} M, concentration of sodium phosphate buffer was 0.092 M, CB[6] was 1.40×10^{-3} M, and CB[7] was 6.79×10^{-4} M.

3. UV-vis spectra of 1 and 2 in the presence of CB[6] and CB[7]

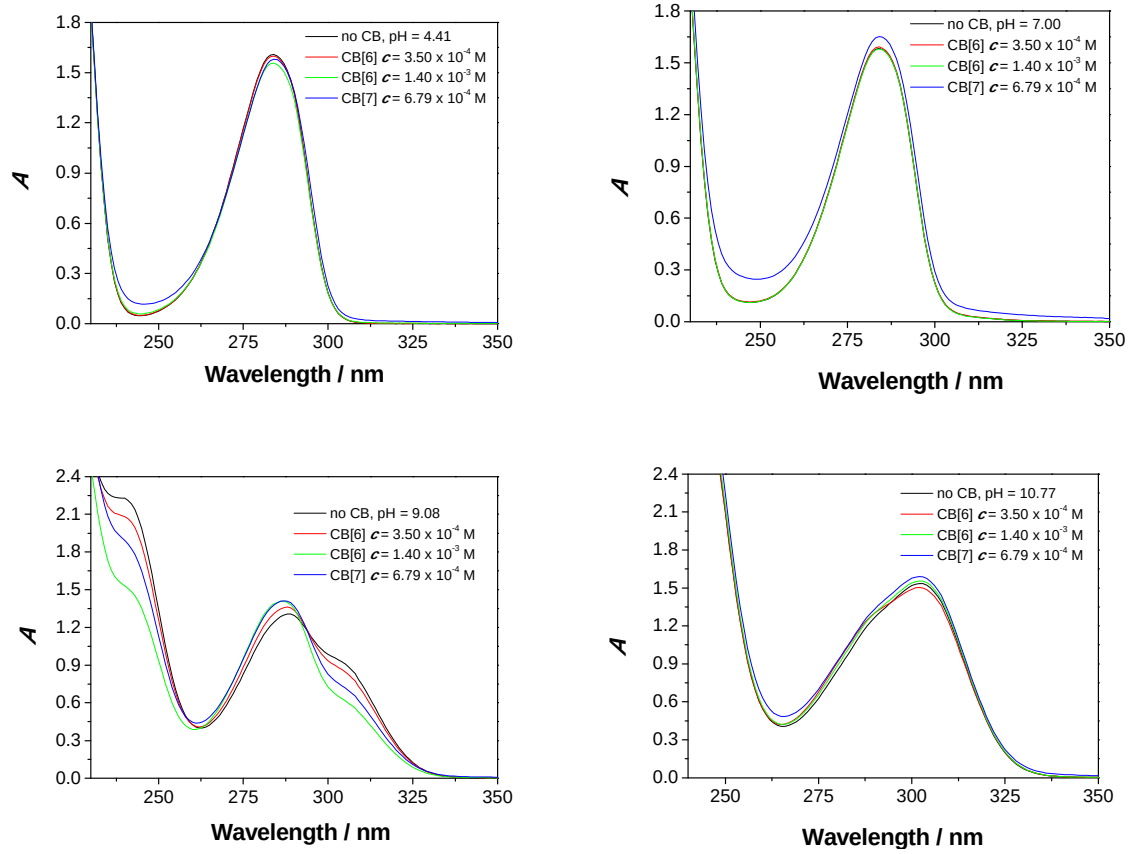

Fig S2. Absorption spectra of **1** (c = 6.35 × 10^{-4} M) in the presence of CB[6] and CB[7] at different pH values.

Absorption spectra of **1** in the presence of CB[6] and CB[7] generally do not reveal large differences. The most pronounced changes were observed at pH 9.08, close to the pK_a value for the phenol deprotonation (pK_{a1} = 8.46).[2] Formation of inclusion complexes is anticipated to change the pK_a value of the guest molecules.[3] Herein, CB[n]s stabilize the positive charge in the salt making molecule **1** less acidic. That is, the pK_a for the phenol deprotonation in the inclusion complex is higher. The higher pK_a is reflected in the changes seen in the spectra at pH 9.08 where on addition of CB[n] the ratio of phenolate *vs*. phenol concentration decreases.

Small changes in the UV-vis spectra on addition of CB[n] to **1** preclude using UV-vis spectroscopy for the determination of binding isotherms. Since the fluorescence of **1** is also very weak, binding constants with CB[n] were determined by microcalorimetry.

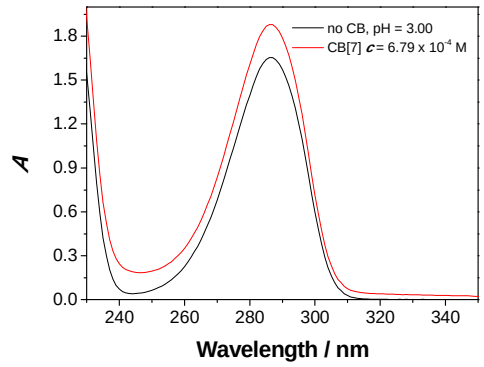
no CB, pH = 3.00
CB[7] c= 6.79 x 10-4 M
A
Wavelength / nm

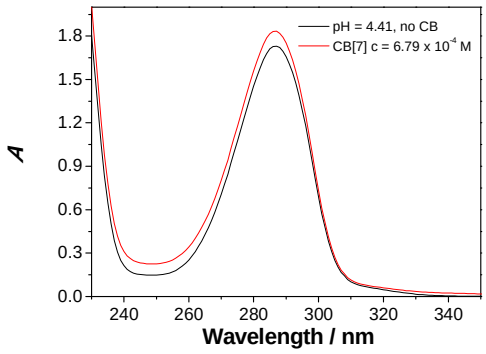
pH = 4.41, no CB
CB[7] c = 6.79 x 10-4 M
A
Wavelength / nm

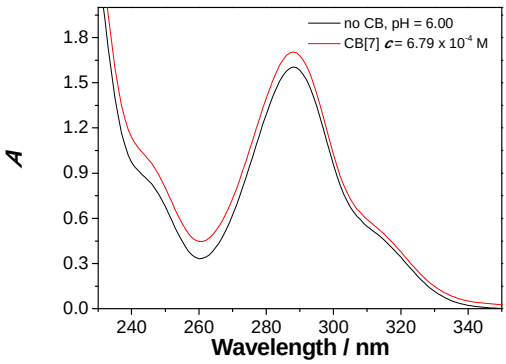
no CB, pH = 6.00
CB[7] c= 6.79 x 10-4 M
A
Wavelength / nm

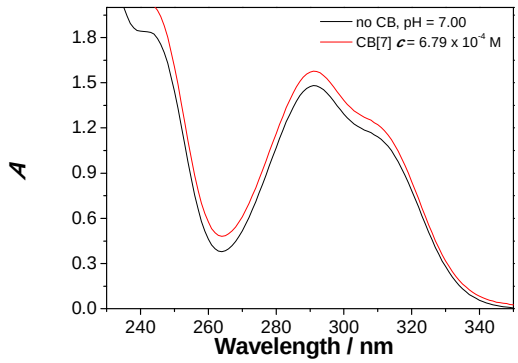
no CB, pH = 7.00
CB[7] c= 6.79 x 10-4 M
A
Wavelength / nm

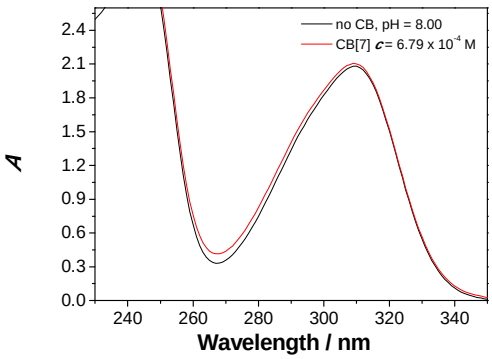
no CB, pH = 8.00
CB[7] c= 6.79 x 10-4 M
A
Wavelength / nm

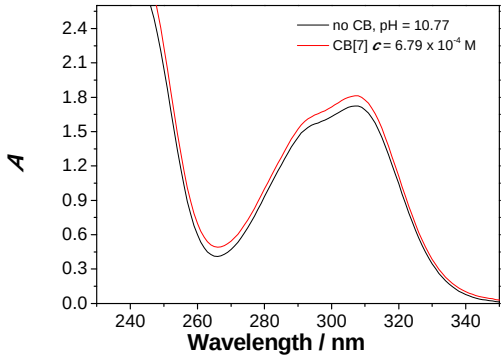
no CB, pH = 10.77
CB[7] c= 6.79 x 10-4 M
A
Wavelength / nm

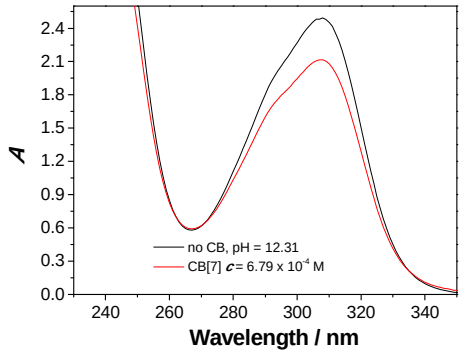

Fig S3. Absorption spectra of **2** (c = 7.6 ×10^{-4} M) in the presence of CB[7] (concentrations of CB[n] not corrected) at different pH values.

Discussion of the UV-vis spectra

Contrary to the results with **1**, addition of CB[n]s to the solution of **2** changed the absorption spectra. CB[7] induced hyperchromic changes in the pH region 3-10, whereas at pH 12, a decrease of the absorbance was observed. The findings suggest that the guest is being bound to CB[n]s.

These results did not indicate changes of pK_a for **2** upon binding with CB[n]s at all pH values with the exception of pH 12. It seems that as long as **2** bears a positive charge, the influence of the CB[n] on its pK_a is not significant. However, at pH 12, $\mathbf{2}^-$ is mostly present in the anionic form, with the phenol and both amines deprotonated. Without CB[n], in the pH region of 10-12 an increase of the absorbance at 308 nm is observed with increasing pH. The decrease of the absorbance in the presence of CB[7] at pH 12 indicates that pK_{a3} of the **2@CB[7]** complex is higher than for the free **2**. That is, **2** is more basic in the CB[n] complex.

4. Prototropic forms for 1 and 2

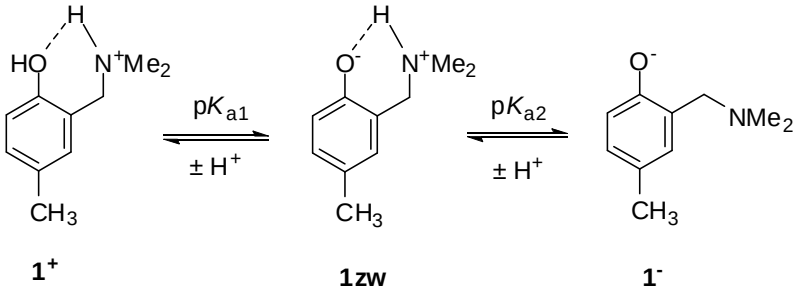

Scheme S1.

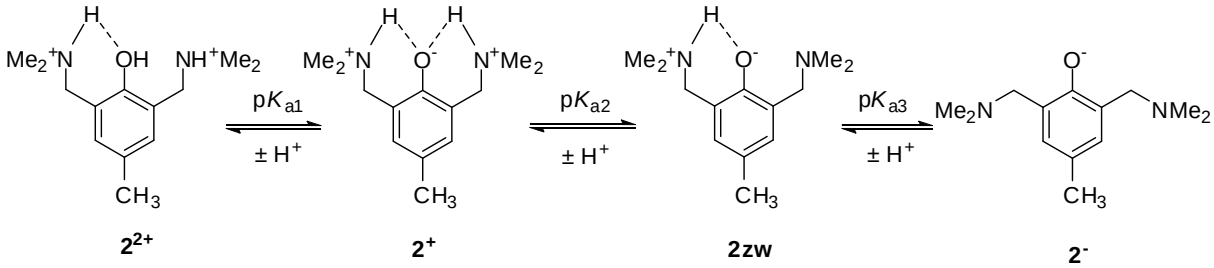

Scheme S2.

Table S1. pK_a values for **1** and **2** in aqueous solution.[a]

Compound	**1**	**2**
pK_{a1}	8.46 ± 0.01	5.87 ± 0.01
pK_{a2}	11.15 ± 0.01	10.00 ± 0.02
pK_{a3}	–	12.31 ± 0.02

[a] Taken from ref. 2

5. Microcalorimetry

The titrations where conducted on a MicroCal VP-ITC Isothermal titration calorimeter (ITC). Before titrations the samples where degassed at 23 °C, 0.4 atm, with stirring at 320 rpm for 10 min. The titrations where performed at 25 °C, with the CB[n] host in the cell and guest in the syringe at 351 rpm. Guests were added in 30-35 injections within the concentration range 1.5-40 mM. The concentration of the CB[n] in the cell was in the range 0.1-0.51 mM. The real concentrations of the CB[n]s used in the experiment were determined by titration.[1]

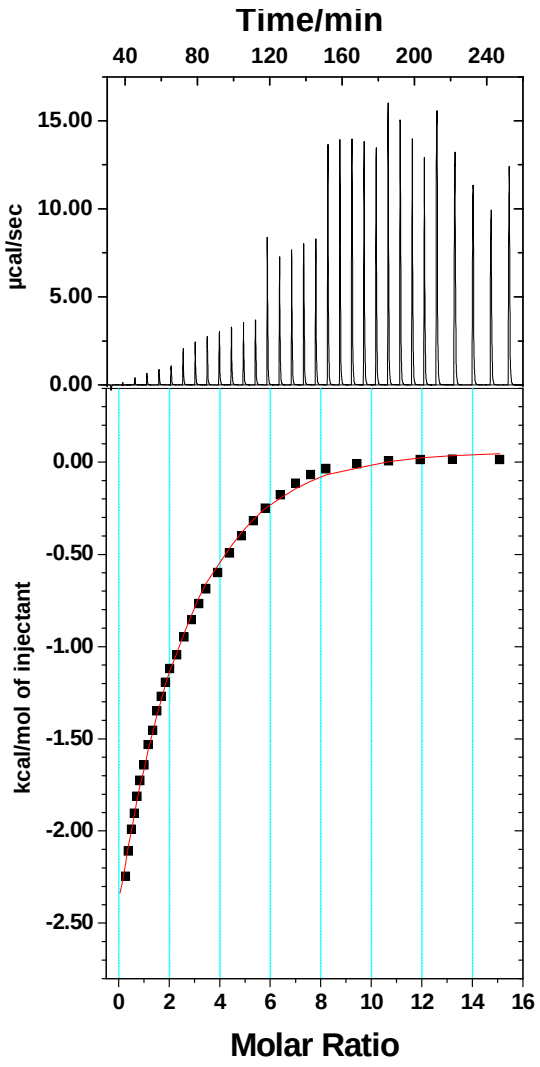

Fig S4. Calorimetric titration of CB[7] (c = 0.5 mM) with **1zw** (c = 40 mM) in H_2O at pH = 9.85 in the presence of phosphate buffer (c = 0.1 M) and NaCl (c = 0.1 M) at 25 °C. Top: raw ITC data; Bottom: dependence of succesive enthalpy change per mol of titrant on **1zw**: CB[7] ratio. The fit shows sistematic deviations indicating the presence of other complexes. The calculated fit is shown as a red line.

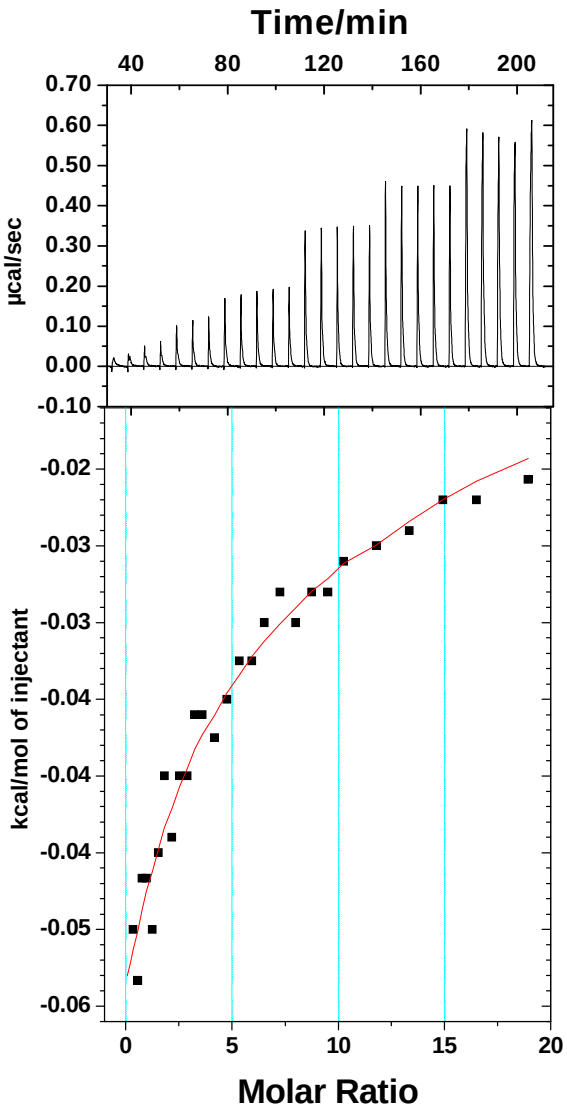

Fig S5. Calorimetric titration of CB[7] (c = 0.5 mM) with $\mathbf{2}^{2+}$ (c = 50 mM) in H_2O at pH = 2.47 in the presence of phosphate buffer (c = 0.1 M) and NaCl (c = 0.1 M) at 25 °C. Top: raw ITC data; Bottom: dependence of succesive enthalpy change per mol of titrant on $\mathbf{2}^{2+}$: CB[7] ratio. The calculated fit is shown as a red line.

Table S2. Thermodynamic parameters for the complexation of **1**$^{+}$, **1zw** and **2**$^{2+}$ with with CB[7].[a]

Complex / pH	K_{11} M^{-1}	ΔH_{11}/ kcal mol^{-1}	ΔS_{11} cal $K^{-1}mol^{-1}$	K_{12} M^{-1}	ΔH_{12}/ kcal mol^{-1}	ΔS_{11} cal $K^{-1}mol^{-1}$
1^{+}@CB[7] pH = 2.47	(5.3±0.3)×10^4	-4.00±0.06	8	(1.00±0.08)× 10^4	1.33±0.08	23
	(5.4±0.5)×10^4	-4.3±0.1	7	(9±1)×10^3	0.3±0.1	17
	(5.3±0.5)×10^4	**-4.2±0.1**	**7.5±0.5**	**(9±1)×10^3**	**1.8±0.5**	**20±3**
1zw@CB[7] pH = 9.83	500±30	-11.7±0.5	-27	230±50	9±1	41
	500±80	-13±2	-31	1100±300	8±2	43
	600±100	-12±1	-27	900±300	7±2	38
	530±100	**-12±1**	**-29±2**	**200-1100**	**8±2**	**41±2**
2^{2+}@CB[7] pH = 2.47	600±200	-0.23±0.06	12	22±6	-2.9±0.6	-4

[a] Titration performed in H_2O at 25 °C in the presence of phosphate buffers and total Na^+ concentration of 0.2 M. The values in bold are the average values from 2 experiments at pH 2.47 and 3 experiments at 9.83.

Binding of the first guest is generally both enthalpically and entropically controlled, except with CB[7] at pH 9.83 where it is only enthalpically controlled, and with CB[6] where entropy control dominates. Binding of the second guest is entropy driven, except for **2**$^{2+}$ with CB[7] where it is only enthalpically controlled.

6. NMR titrations and NOESY experiments

All concentrations of CB[n]s reported in this paragraph are corrected based on titration.[1]

The 0.1 M solutions of deuteriophosphate buffers were prepared by mixing an appropriate amount of 40% NaOD and 85% D_3PO_4 in D_2O. To each buffer, NaCl was added in the concentration of 0.1 M to solubilize CB[n]s. pH values were measured for each buffer. pD values can be calculated according to the formula:[4]

pD = pH (reading) + 0.41

For compound **1**, one NMR titration with CB[6] was performed at pH 2.63, and three NMR titrations with CB[7] at pH 2.63, 9.25 and 12.50. pH values were selected so that one type of prototropic species is dominant, $\mathbf{1}^+$, **1zw** or $\mathbf{1}^-$ (see Scheme S1 above).

Table S3. Conditions in the NMR titration of CB[6] with $\mathbf{1}^+$.

Measured pH (calculated pD)	5.60 (6.01)
c ($\mathbf{1}^+$) / M	6×10^{-3}
c (CB[6]) / M	1×10^{-2}
c (sodium deuteriophosphates) / M	0.1 (NaD_2PO_4)
c (Na^+ total) / M = *c*(phosphate) + *c*(NaCl)	0.2
NMR titration experimental details	Aliquots of a compound **1** solution were added to 0.5 mL of CB[6] solution in a NMR tube. After each addition, a NMR spectrum was recorded. [H] / [G] ratio varied from 100 to 0.2

Table S4. Conditions in the NMR titrations of CB[7] with **1**.

Measured pH (calculated pD)	2.63 (3.04)	9.25 (9.66)	12.50 (12.91)
c (**1**$^+$**/1zw/1**$^-$) / M	6×10^{-3}	4×10^{-2}	4×10^{-2}
c (CB[7]) / M	3.45×10^{-3}	1.02×10^{-2}	0.978×10^{-2}
c (sodium deuteriophosphates) / M	0.1 (D_3PO_4-NaD_2PO_4)	0.1 (Na_2DPO_4)	0.1 (Na_3PO_4)
c (Na^+ total) / M = *c*(phosphate) + *c*(NaCl)	0.2	0.3	0.4
NMR titration experimental details	Aliquots of compound **1** solution were added to 0.5 mL of CB[7] solution in a NMR tube. After each addition, a NMR spectrum was recorded. [H] / [G] ratio varied from 34.6 to 0.054	Aliquots of compound **1** solution were added to 0.5 mL of CB[7] solution in a NMR tube. After each addition, a NMR spectrum was recorded. [H] / [G] ratio varied from 50.8 to 0.10	Aliquots of compound **1** solution were added to 0.5 mL of CB[7] solution in a NMR tube. After each addition, a NMR spectrum was recorded. [H] / [G] ratio varied from 48.9 to 0.098

NMR spectra from titrations

1$^+$ + CB[6], pH = 5.59

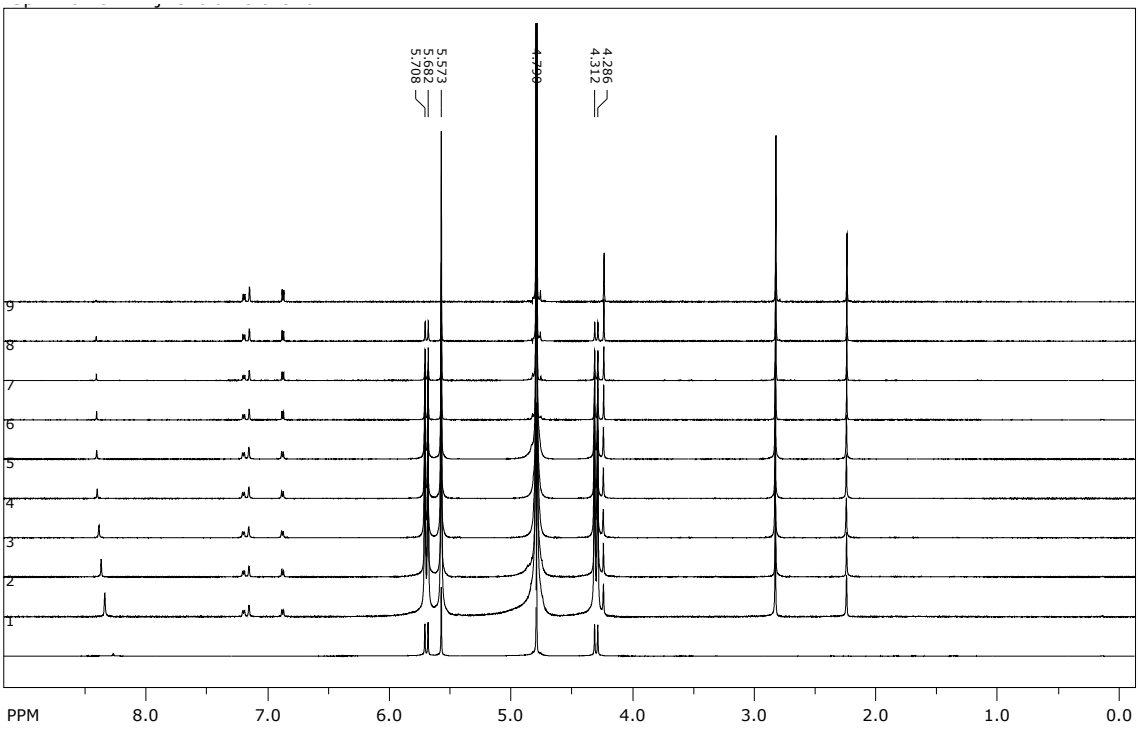

Fig S6. Spectra from the NMR titration of CB[6] with **1**$^+$. Aliquots of the solution containing **1**$^+$ (c = 6×10^{-3} M) were added to the CB[6] solution (0.5 mL, c = 1×10^{-2} M) in a NMR tube. NaCl (c = 0.1 M) was added to solubilize CB[6]. The solution was buffered with NaD_2PO_4 (c = 0.1 M). Total $c(Na^+)$ = 0.2 M.

Table S5. Legend for Fig S6 (spectra) shown above.

№ of spectra on Fig S6	c(CB[6]) / c(**1**$^+$)
9	Compound **1**$^+$ only
8	0.2
7	0.4
6	0.6
5	0.8
4	1
3	1.5
2	2
1	4
0	CB[6] only

NOESY spectra were recorded for compounds $\mathbf{1}^{+}$ and $\mathbf{2}^{2+}$ in the presence of CB[n].

Conditions:

c(compound) = 1×10^{-3} M

c(CB[n]) = 3×10^{-3} M

Compounds were dissolved in D_2O, buffered with NaD_2PO_4-D_3PO_4 (0.1 M) to pH 2.5 (pD 2.9) + 0.1 M NaCl (total 0.2 M Na^{+}).

Spectra were recorded at 300 MHz.

The results were compiled in the Table S9. Interactions between higher field doublet of CB[6] or CB[7] (proton H_{out}) and compound protons should be taken with a caution, because methylene (CH_2) signal of the compound **1** or **2** and the doublet of CB[n]'s H_{out} overlap. That is marked with (?) in Table S7.

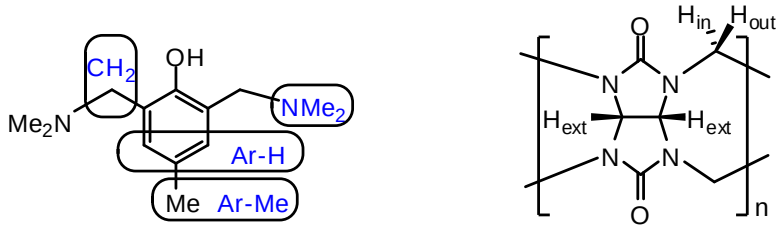

Fig S7. Common abbreviations for the H-atoms used in this report. H_{in} - facing the CB[n] cavity, H_{out} - facing away from the CB[n] cavity, H_{ext} - external protons of CB[n], those on the central rim of the CB[n]. If they are resolved, H atoms from the benzene ring are marked with the number that corresponds to their position on the benzene ring (OH group is on the carbon 1).

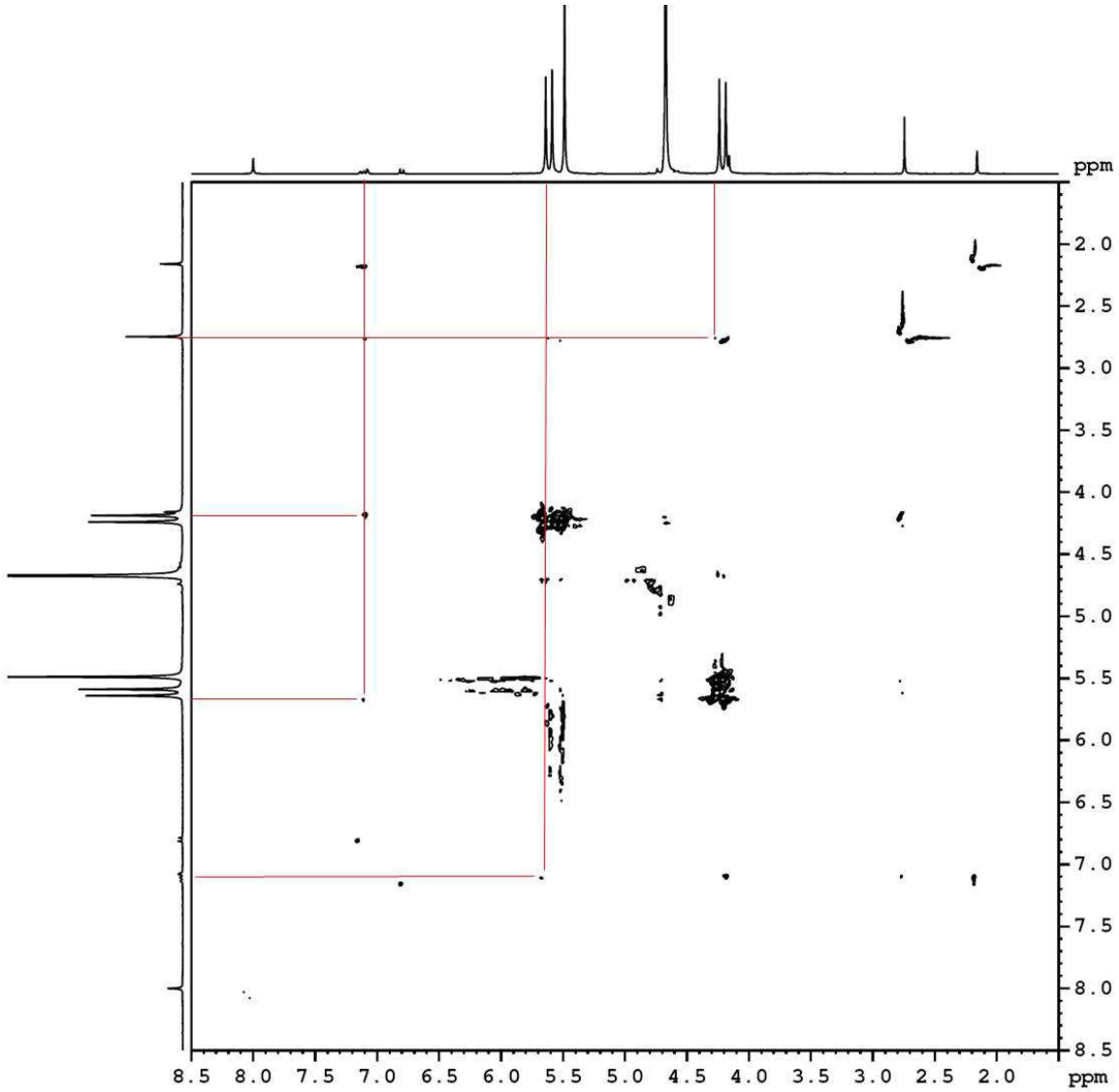

Fig S8. NOESY spectrum of $\mathbf{1}^+$ (c = 1×10^{-3} M) + CB[6] (c = 3×10^{-3} M) at pH 2.40. NaCl (c = 0.1 M) was added to solubilize CB[6]. The solution was buffered with NaD_2PO_4-D_3PO_4 (c = 0.1 M). Total $c(Na^+)$ = 0.2 M.

Dimensions of inner cavity, height and width of the CB[6] and CB[7] were taken from reference 5 and used in the discussion. Dimensions of molecules $\mathbf{1}^{+}$ and $\mathbf{2}^{2+}$ were calculated by B3LYP/6-31G(d,p) level of theory using Gaussian 09 program.[6]

	Structure	**Structure, top view**
$\mathbf{1}^{+}$-*syn*	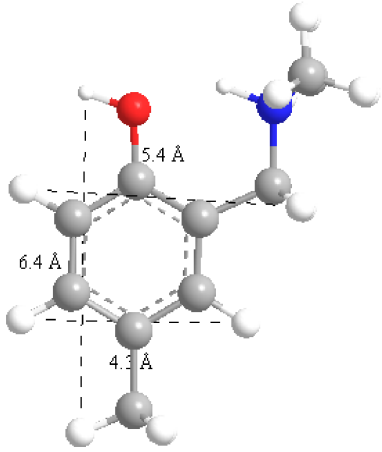	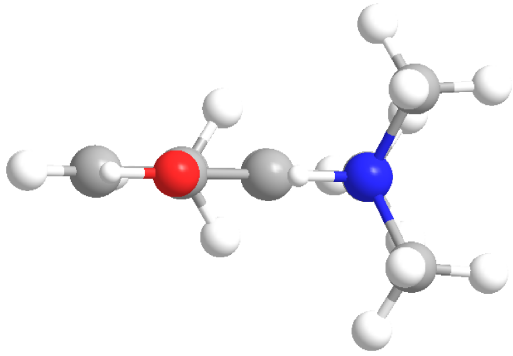
$\mathbf{1}^{+}$-*anti*	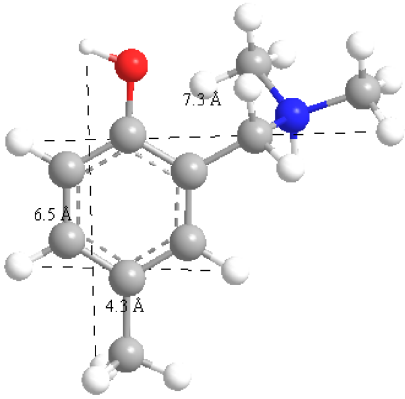	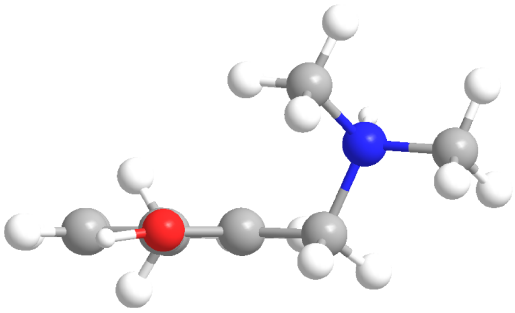

Fig S9. Calculated distances for compound $\mathbf{1}^{+}$, at B3LYP/6-31G(d,p) level of theory.

The shortest width of molecule $\mathbf{1}^{+}$ is 4.3 Å (between the hydrogens at the positions 3- and 5- on the benzene ring), which is larger than the width of the CB[6] cavity (3.9 Å), but smaller than the width of CB[7] (5.4 Å). It is known that only *para* substituted compounds can enter CB[6] cavity, whereas *o*- or *m*- substituted derivatives do not form inclusion complexes.[7] In compound $\mathbf{1}^{+}$ three substituents on the benzene ring exist, preventing $\mathbf{1}^{+}$ to form the inclusion complex with

CB[6]. However, $\mathbf{1}^{+}$ can fit in the CB[7] cavity (molecule width 5.4 Å, CB[7] cavity width 5.4 Å). The formation of the inclusion complex **1**@CB[7] is anticipated and supported by NMR titrations (*vide supra*).

	Structure	**Structure, top view**
$\mathbf{2}^{2+}$-*syn-syn trans*	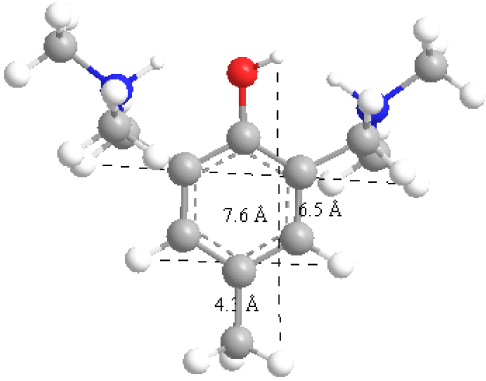	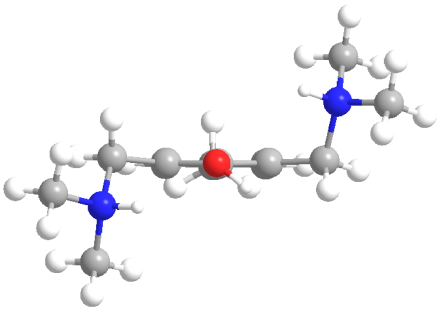
$\mathbf{2}^{2+}$-*syn-anti cis*	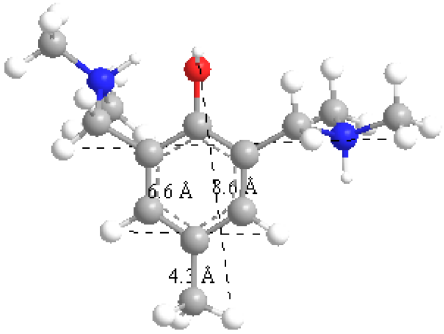	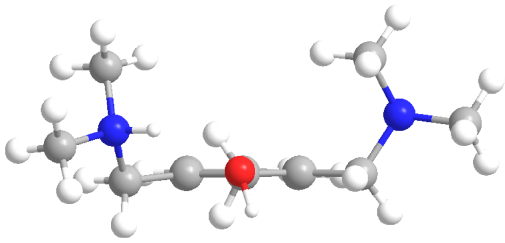
$\mathbf{2}^{2+}$-*syn-syn cis*	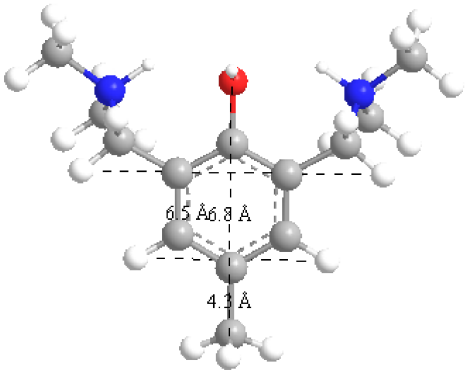	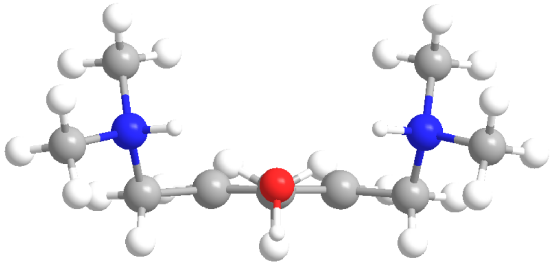

2^{2+}-*anti-anti trans*	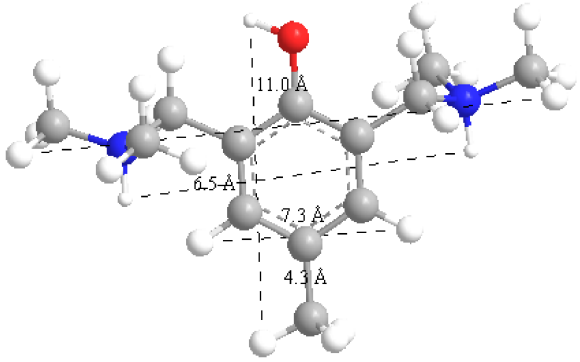	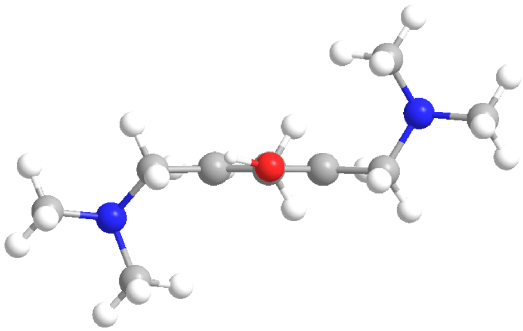

Fig S10. Calculated distances for compound **2**$^{2+}$, at B3LYP/6-31G(d,p) level of theory.

Molecule **2**$^{2+}$ is bigger than **1**$^{+}$. Therefore, **2**$^{2+}$ can only form an external complex with CB[6] and maybe some type of the inclusion complex with CB[7]. $CH_2 \cdots CH_2$ distances (~6.5 Å) in all conformers of **2**$^{2+}$ are larger than the CB[7] cavity (5.4 Å), indicating that the whole molecule cannot fit in the cavity, but can form a complex where a part of the molecule enters the cavity, whereas protonated amino-groups form hydrogen bonds with the CB[7] rim. Thus, a half of the molecule is immersed in the CB[7] cavity, leaving place on the other side of the CB[7] free to accept another molecule **2**$^{2+}$ and give a complex with the 1:2 (CB[7] : **2**$^{2+}$) stoichiometry.

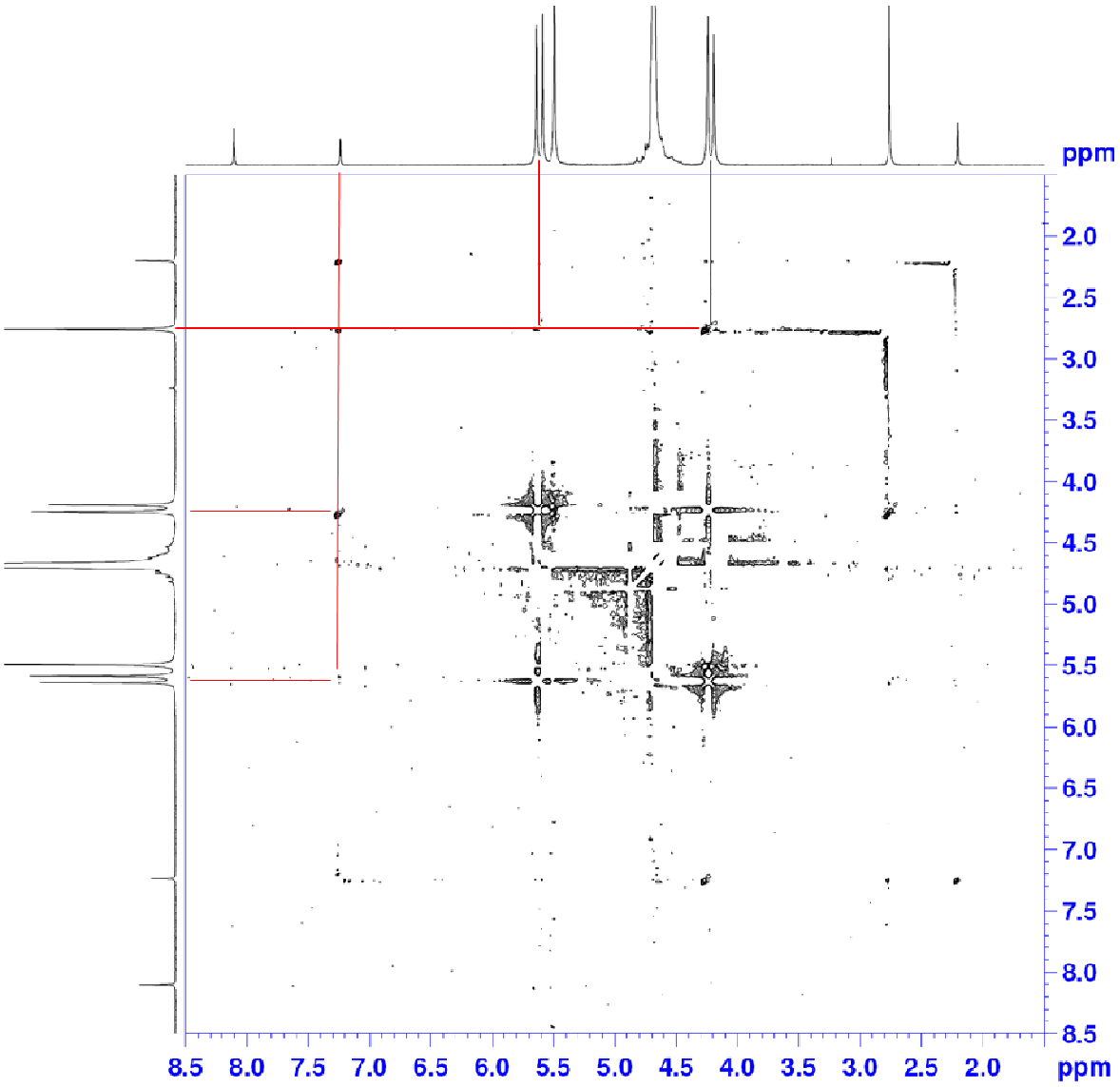

Fig S11. NOESY spectrum of compound $\mathbf{2}^{2+}$ (c = 1×10^{-3} M) + CB[6] (c = 3×10^{-3} M) at pH 2.47. NaCl (c = 0.1 M) was added to solubilize CB[6]. The solution was buffered with NaD_2PO_4-D_3PO_4 (c = 0.1 M). Total $c(Na^+)$ = 0.2 M.

1^{+}+ CB[7], pH = 2.63

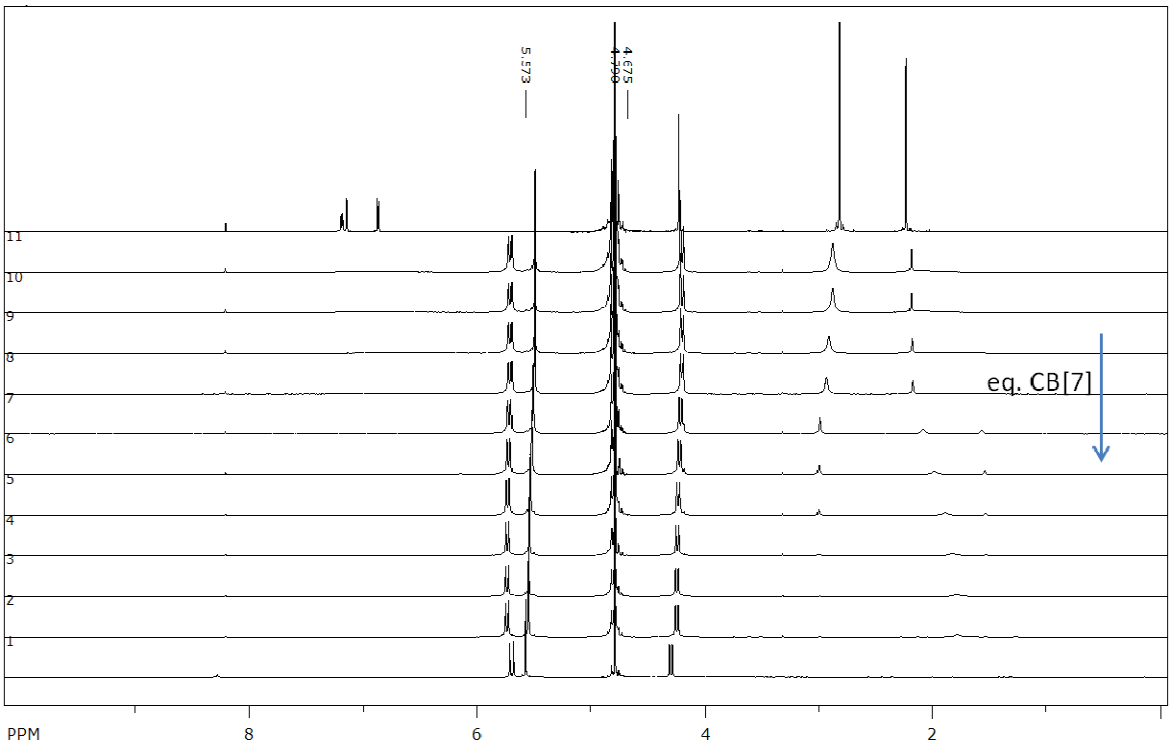

Fig S12. Spectra from the NMR titration of CB[7] with **1**$^{+}$. Aliquots of solution containing **1**$^{+}$ (c = 6×10^{-3} M) were added to the of CB[7] solution (0.5 mL, c = 3.45×10^{-3} M) in a NMR tube. NaCl (c = 0.1 M) was added to solubilize CB[7]. The solution was buffered with NaD_2PO_4-D_3PO_4 (c = 0.1 M). Total c(Na^+) = 0.2 M.

Table S6. Legend for Fig S12 (spectra) shown above.

№ of spectra on fig S12	c(CB[7]) / c(**1**$^{+}$)
11	Compound **1**$^{+}$ only
10	0.054
9	0.099
8	0.229
7	0.432
6	0.943
5	1.60
4	2.93
3	6.19
2	19.7
1	34.6
0	CB[7] only

1$^+$, pH = 2.63

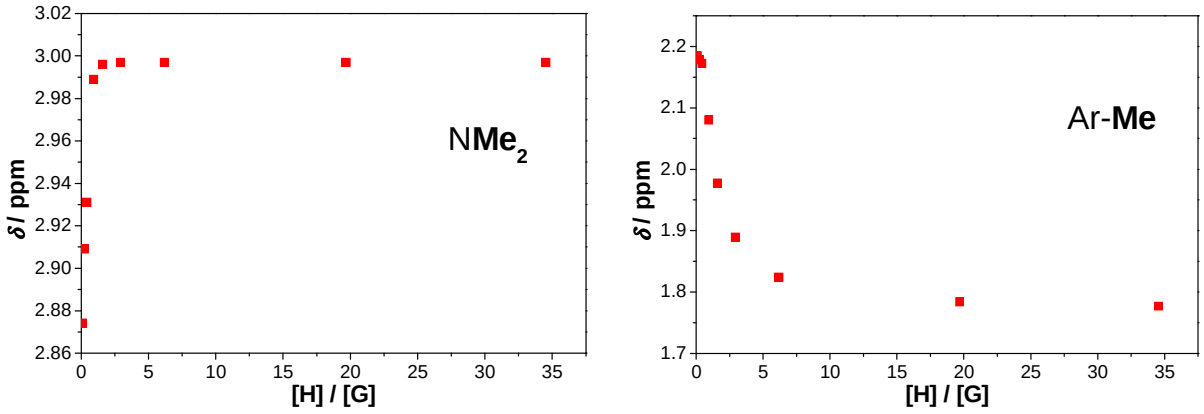

Fig S13. Dependence of the chemical shift of given protons in molecule **1**$^+$ (on CB[7] : **1**$^+$ ratio) in the titration of CB[7] with **1**$^+$ at pH 2.63.

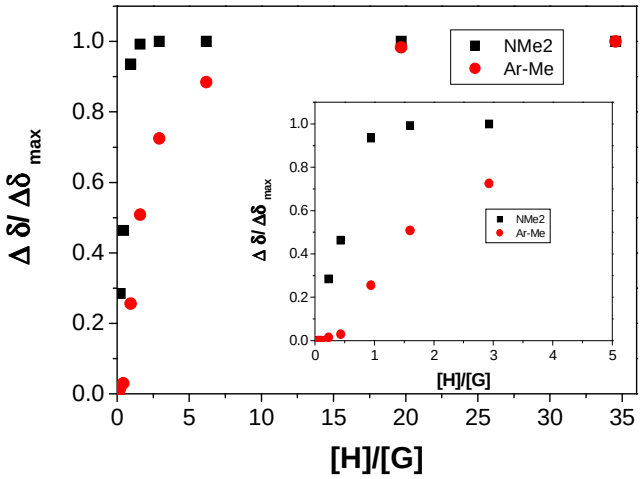

Fig S14. Dependence of the normalized difference of chemical shift of given protons in molecule **1**$^+$ (on CB[7] : **1**$^+$ ratio) in the titration of CB[7] with **1**$^+$ at pH 2.63; Inset: enlarged region of the plot for the CB[7] : **1**$^+$ in the range 0-5.

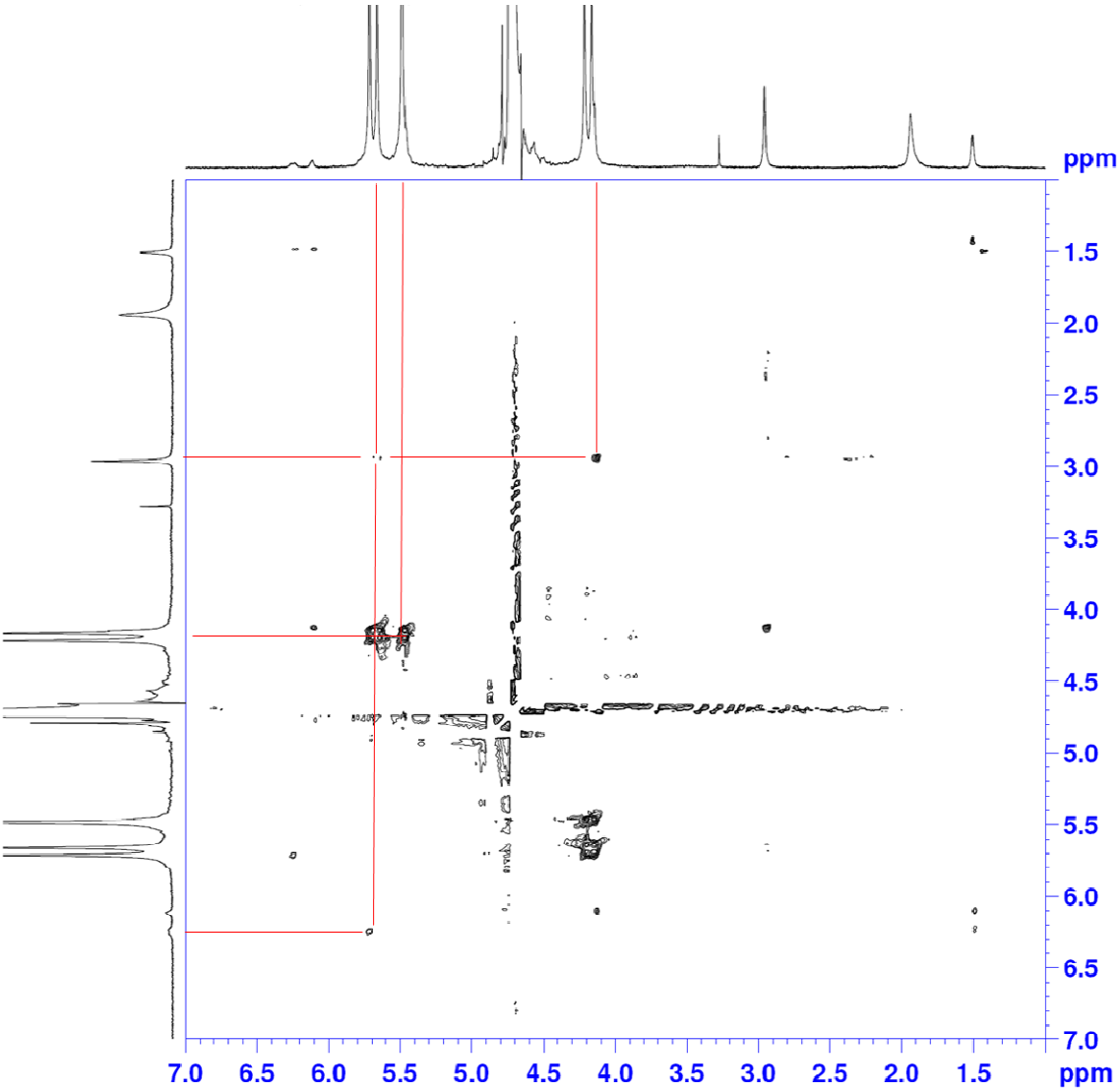

Fig S15. NOESY spectrum of compound $\mathbf{1}^+$ (c = 1×10^{-3} M) + CB[7] (c = 3×10^{-3} M) at pH 2.47. NaCl (c = 0.1 M) was added to solubilize CB[7]. The solution was buffered with NaD_2PO_4-D_3PO_4 (c = 0.1 M). Total c(Na^+) = 0.2 M.

Table S7. List of important NOE interactions between the guest H-atoms and CB[7] H-atoms.

Compound	pH →	2.47	9.66	12.5
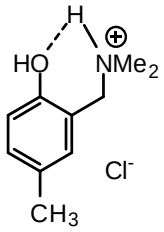 **1**		$NMe_2\cdots H_{out}$ (?) $NMe_2\cdots H_{in}$ Ar-H$\cdots H_{in}$ Ar-H$\cdots H_{out}$ **(?)** 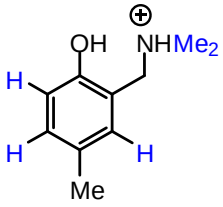 Spectrum – see Fig S17	Ar-Me$\cdots H_a$ Ar-Me$\cdots H_b$ Ar-Me$\cdots H_c$ 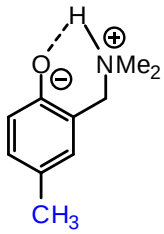	NOE signal between the compound protons and CB[7] protons were not observed

Compound	pH →	2.5	7.75	12.7
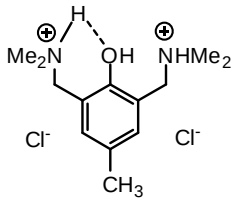 **2**	H/G = 1:1 Ar-H$\cdots H_{out}$ (?) $NMe_2\cdots H_{out}$ $NMe_2\cdots H_{in}$ $NMe_2\cdots H_{ext}$ 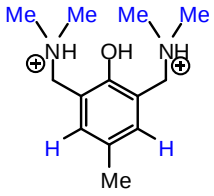 H/G = 1:2 Ar-H$\cdots H_{out}$ (?) $NMe_2\cdots H_{out}$ (?) $NMe_2\cdots H_{ext}$ $NMe_2\cdots H_{in}$ 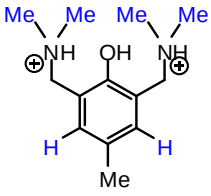	Ar-H$\cdots H_{out}$ (??) $NMe_2\cdots H_{out}$ (??) 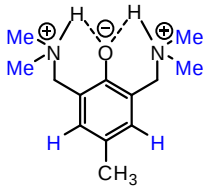	NOE signal between the compound protons and CB[7] protons were not observed.

Fitting of the NMR titration data

Fitting of the NMR titration data was carried out by P. Thordarson's program for global analysis freely available on internet.[8] The best fit to the model H:G = 1:2 was obtained for the titration of CB[7] with compound $\mathbf{1}^+$ in acidic solution (pH = 2.63, pD = 3.04). However, the binding constants were revealed with large errors, K_{11} = 2.0×10^5 M^{-1} (278%) and K_{12} = 800 M^{-1} (109%), where the confidence interval for the binding constant (% from asymptotic error) is given in parentheses. Large errors are due to the presence of other complexes in the solution, so the model H:G = 1:2 is not adequate. Formation of complexes with 1:1 and 1:2 stoichiometries were also indicated by isothermal microcalorimetric titrations (*vide supra*) where better quality of the fits allowed for the precise determination of the binding isotherm parameters.

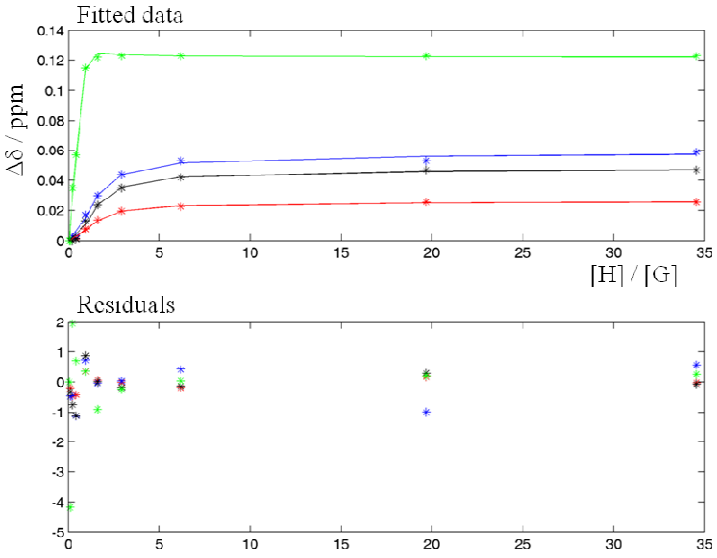

Fig S16. Data from the titration of CB[7] with $\mathbf{1}^+$ at pH 2.63. The top graph reports difference in chemical shift for signals: NC**H**$_3$ (green), CB[7] singlet (blue), CB[7] doublet (black) and CB[7] doublet (red). *vs.* [H]/[G] ratio. * are the experimental values, — is calculated fit to the model involving complex stoichiometries H:G = 1:1 and H:G = 1:2. In the bottom graph, residuals (difference between the experimental and the calculated value) are plotted *vs.* [H]/[G] ratio.

1zw + CB[7], pH = 9.25

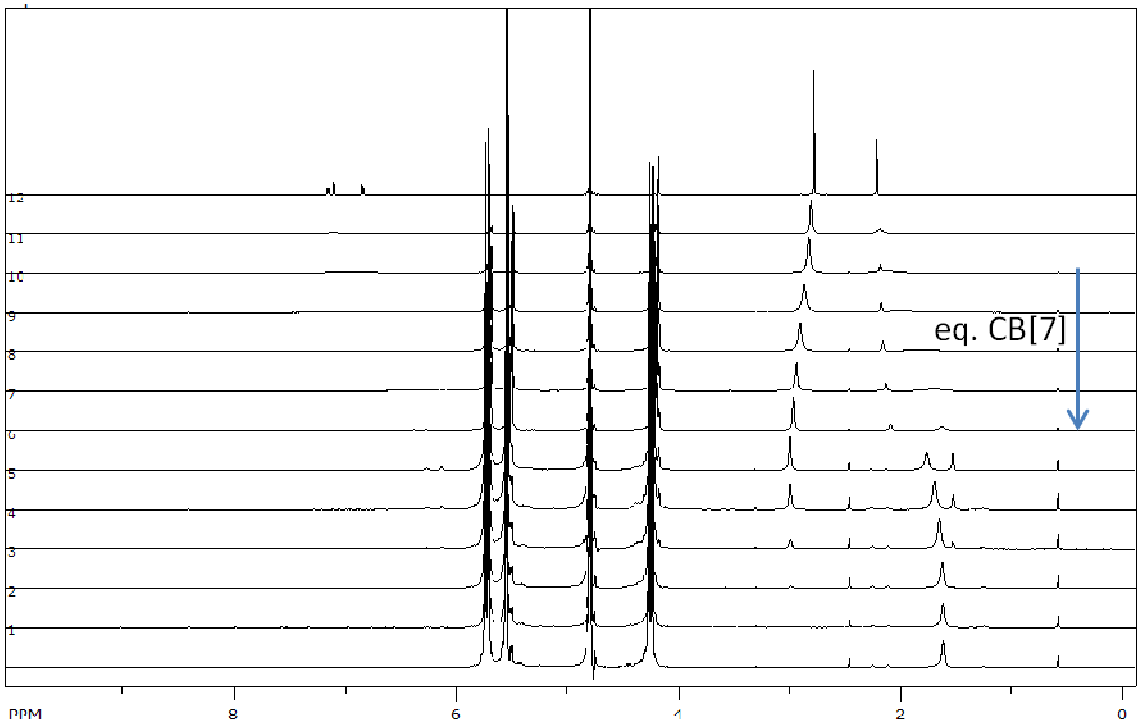

Fig S17. Spectra from NMR titration of CB[7] with **1zw**. Aliquots of solution containing **1** (c = 4×10^{-2} M) were added to the CB[7] solution (0.5 mL, c = 1.02×10^{-2} M) in a NMR tube. NaCl (c = 0.1 M) was added to solubilize CB[7]. The solution was buffered with Na_2PO_4 (c = 0.1 M). Total $c(Na^+)$ = 0.3 mol dm^{-3}.

Table S8. Legend for Fig S17 (spectra) shown above.

№ of spectra on fig S17	c(CB[7]) / c(**1zw**)
12	Compound **1zw** only
11	0.102
10	0.203
9	0.406
8	0.609
7	0.812
6	1.02
5	3.04
4	5.08
3	10.2
2	30.2
1	50.8
0	CB[7] only

1zw, pH = 9.25

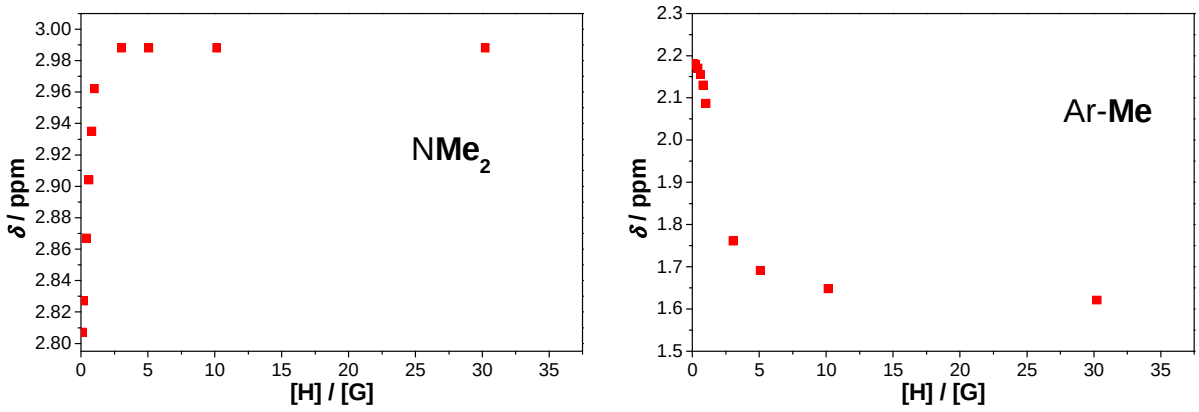

Fig S18. Dependence of the chemical shift of given protons in molecule **1** (on CB[7] : **1** ratio) in the titration of CB[7] with **1zw** at pH 9.25.

Discussion of the results obtained by NMR titrations of CB[7] with 1

The trends in the chemical shift changes for compound **1** at different concentrations of CB[7] and different pH values are shown in Figs. S13 and S18. NMe_2 and Ar-Me protons follows the same trend for protonated, positively charged $\mathbf{1}^+$, and zwitterionic **1zw**. That leads to the conclusion that the binding mode of cationic $\mathbf{1}^+$ and zwitterionic **1zw** to CB[7] is probably the same. In addition to the changes of chemical shifts, a significant line-broadening of the Ar-H signals in ^{1}H NMR spectra of $\mathbf{1}^+$ and **1zw** was observed in presence of CB[7], even when a ratio of CB[7] : **1** was very small (see figs S12 and S17).

Considering the magnetic properties of the carbonyl groups at the CB[7] portals, we propose the following geometry for **1**@CB[7]. In all cases, CB[7] protons are deshielded upon complexation, in line with the formation of inclusion complexes. CB[n] protons in the complex face the hydrogens of the benzene ring (not strictly applicable to H_{ext}).

Upon binding of the prototopic species $\mathbf{1}^+$ and **1zw** to CB[7], the signals corresponding to $N(CH_3)_2$ are deshielded, whereas Ar-CH_3 protons are shielded. Ar-H protons are also shielded in the complex, but a significant line broadening takes place, so their chemical shifts are not available. The trend of the signals change suggests that the $N(CH_3)_2$ protons in **1** are above the CB[7] rim and form electrostatic interactions with the carbonyl groups. On the contrary, Ar-Me and Ar-H protons are in the cavity, below the CB[7] carbonyl group rim. The observed trends in

the spectra upon titration are fully in accord with the formation of inclusion complex at pH < 9.25 as shown in Fig. S19.

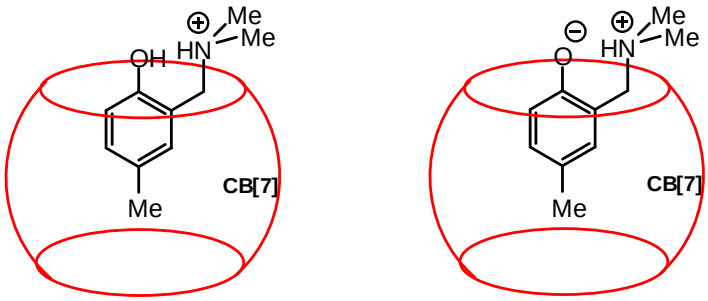

1^{+}@CB[7] **1zw**@CB[7]

Fig. S19. Structure of complexes of **1**$^{+}$ and **1zw** with CB[7].

NMR titrations with 2 and CB[7]

The titrations with **2** and CB[7] were performed at pH 2.51, 7.75 and 12.7. The pH values were selected so that one type of the prototrophic form dominates, dicationic $\mathbf{2}^{2+}$, monocationic $\mathbf{2}^{+}$, neutral zwitterionic **2zw**, and anionic $\mathbf{2}^{-}$ (see Scheme S2).

Table S9. Conditions in the NMR titrations of CB[7] with **2**.

Measured pH (calculated pD)	2.51 (2.92)	7.75 (8.16)	12.7 (13.1)
c ($\mathbf{2}^{2+}$/$\mathbf{2}^{+}$/**2zw**) / M	4×10^{-2}	4×10^{-2}	4×10^{-2}
c (CB[7]) / M	1.17×10^{-2}	1.13×10^{-2}	8.86×10^{-3}
c (sodium deuteriophosphates) / M	0.1 (D_3PO_4-NaD_2PO_4)	0.1 (Na_2DPO_4)	0.1 (Na_3PO_4)
c (total Na^+) / M = *c*(phosphate) + *c*(NaCl)	0.2	0.3	0.4
NMR titration experimental details	Aliquots of compound **2** solution were added to 0.5 mL of CB[7] solution in a NMR tube. After each addition, a NMR spectrum was recorded. [H] / [G] ratio form 58.4 to 0.117	Aliquots of compound **2** solution were added to 0.5 mL of CB[7] solution in a NMR tube. After each addition, a NMR spectrum was recorded. [H] / [G] ratio form 56.4 to 0.113	Aliquots of compound **2** solution were added to 0.5 mL of CB[7] solution in a NMR tube. After each addition, a NMR spectrum was recorded. [H] / [G] ratio form 44.3 to 0.089

$\mathbf{2}^{2+}$ + CB[7], pH = 2.51

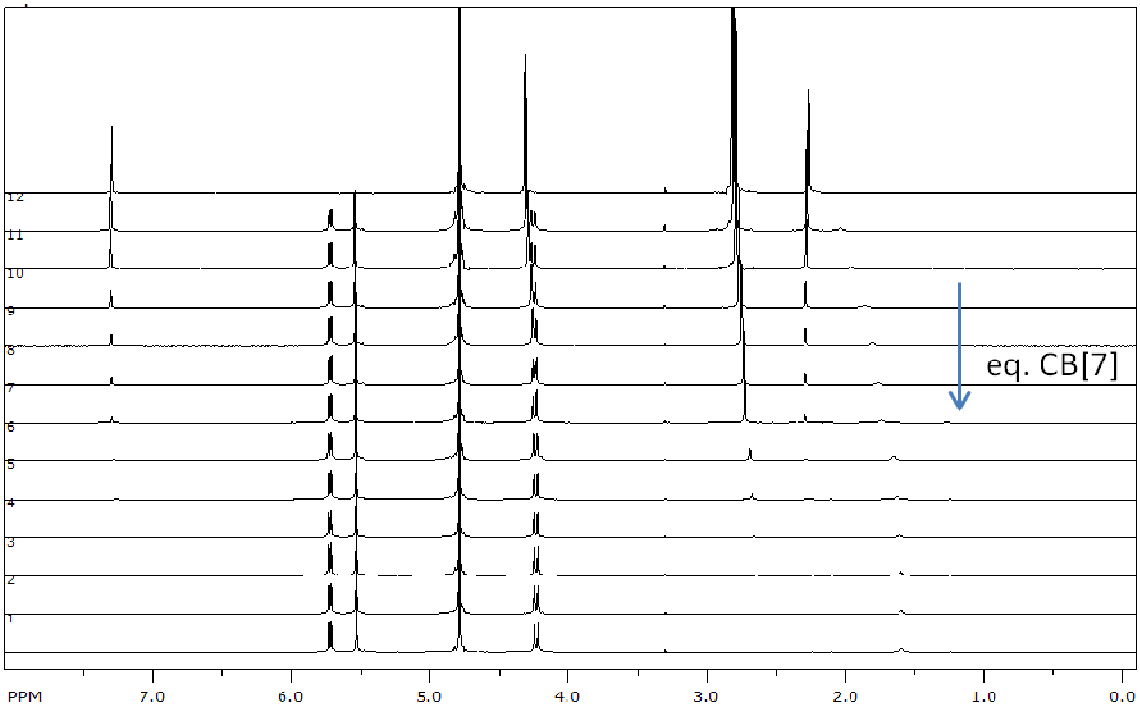

Fig S20. Spectra from NMR titration of CB[7] with $\mathbf{2}^{2+}$. Aliquots of solution containing **2** (c = 4×10^{-2} M) were added to the CB[7] solution (0.5 mL, c = 1.17×10^{-2} M) in a NMR tube. NaCl (c = 0.1 M) was added to solubilize CB[7]. The solution was buffered with NaD_2PO_4-D_3PO_4 (c = 0.1 M). Total $c(Na^+)$ = 0.2 M.

Table S10. Legend for Fig S20 (spectra) shown above.

№ of spectra on fig S20	c(CB[7]) / $\mathbf{2}^{2+}$
12	Compound $\mathbf{2}^{2+}$ only
11	0.117
10	0.234
9	0.467
8	0.701
7	0.934
6	1.17
5	3.50
4	5.84
3	11.7
2	34.8
1	58.4
0	CB[7] only

$\mathbf{2}^{2+}$, pH = 2.51

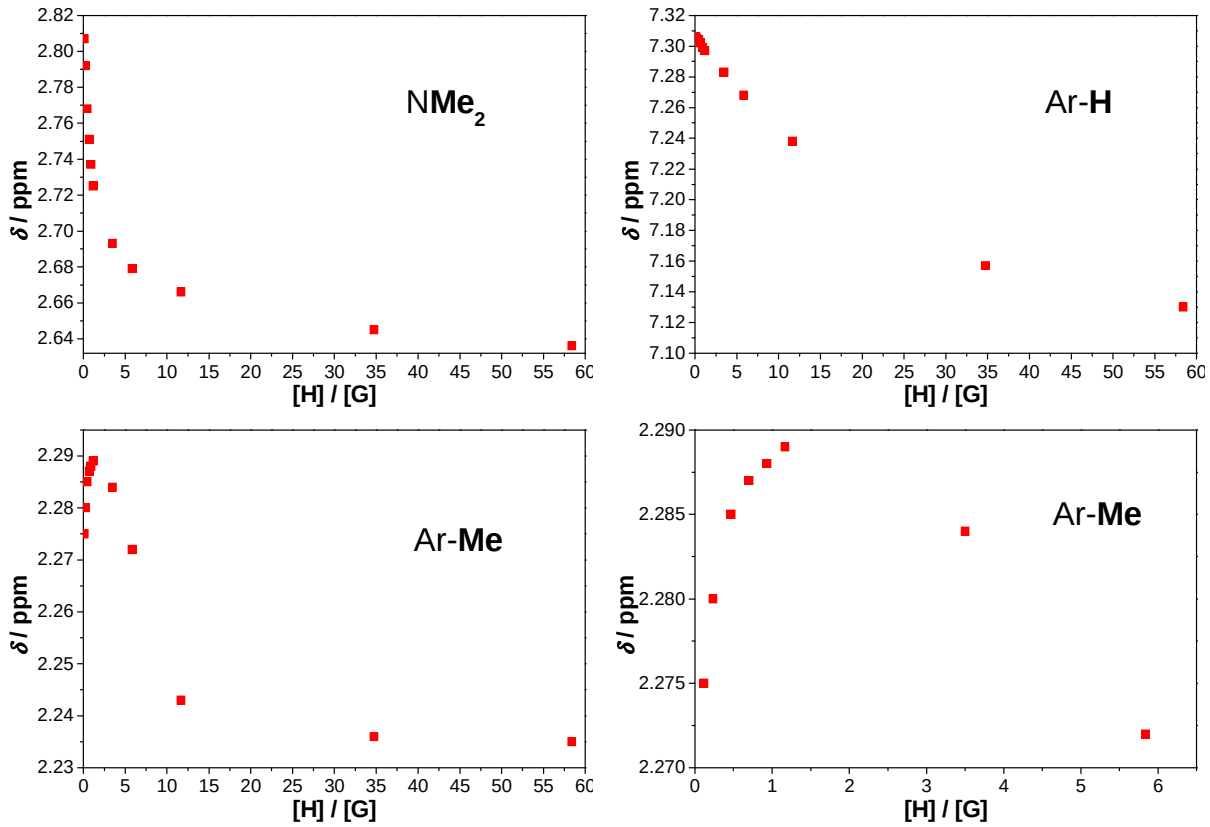

Fig S21. Dependence of the chemical shift of given protons in molecule $\mathbf{2}^{2+}$ (on CB[7] : $\mathbf{2}^{2+}$ ratio) in the titration of CB[7] with $\mathbf{2}^{2+}$ at pH 2.51. There is a different trend for Ar-Me protons in [H]/[G] range 0-2.

Discussion of the results obtained by NMR titrations of CB[7] with $\mathbf{2}^{2+}$

Signals of the CB[7] protons were not affected during the titration, except at pH 2.51 (dication is the predominant species) when very small changes in the chemical shift of the CB[7] protons were observed. On the contrary, chemical shifts of $\mathbf{2}^{2+}$ change in the titrations at all pH values. The finding suggests formation of the inclusion complex between CB[7] and $\mathbf{2}^{2+}$ at pH 2.51 and exclusion complexes at other pH values. Furthermore, the protons of $\mathbf{2}^{2+}$ are shielded upon complexation, except for the Ar-Me protons in the acidic solution ($\mathbf{2}^{2+}$, pH = 2.51, Fig. S21 bottom left and right) where different trends were observed depending on the host concentration. At low CB[7] concentrations, the Ar-$\mathbf{CH_3}$ signals experienced deshielding, whereas at higher

CB[7] concentrations they are shielded (Figs. S20 and S21). This observation was rationalized by the formation of complexes with 1:1 and 1:2 (H:G) stoichiometries. The shielding effect is due to the formation of 1:1 inclusion complex, whereas deshielding results from the anisotropic effect of one aryl ring to the methyl group of the other molecule in the 1:2 complex (Fig. S22). Chemical shifts of the other protons in $\mathbf{2}^{2+}$ do not follow the same trend during titration as Ar-Me signals. At higher ratios of CB[7] to $\mathbf{2}^{2+}$, only shielding of the signals was induced, as shown in Fig. S21.

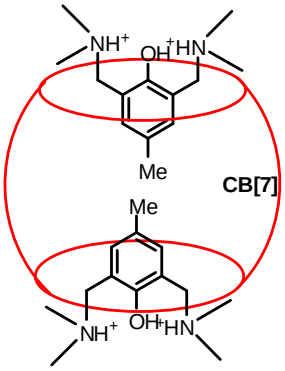

Fig S22. Complex of CB[7] with two molecules of $\mathbf{2}^{2+}$.

Ar-Me protons are deshielded upon addition of CB[7] until the ratio of CB[7]: $\mathbf{2}^{2+}$ = 2:1 is reached. However, at higher concentration of CB[7], the Ar-Me signal is shielded. The finding can be explained in the light of the theory of molecular currents.[9] At low CB[7] concentration (CB[7]: $\mathbf{2}^{2+}$ < 1:2), the dominant complex has 1:2 stoichiometry (CB: $\mathbf{2}^{2+}$). Protons which are in the plane with the benzene ring are deshielded. Thus, both Ar-Me groups feel the deshielding effect of the molecular current from the neighboring benzene ring.[9] At a higher CB[7] concentration, the complex with 1:1 stoichiometry becomes predominant species. In the 1:1 complex, the Ar-Me group does not have another benzene ring in the proximity, so the carbonyl groups of CB[7] have the predominant shielding effect on its chemical shift.

8. Laser Flash Photolysis (LFP)

All LFP studies were performed on a system previously described[10] using as an excitation source a pulsed Nd:YAG laser at 266 nm (<20 mJ per pulse), with a pulse width of 10 ns. Static cells (7 mm × 7 mm) were used. The absorbances of the solutions were in the range A_{266} = 0.28 - 0.37. In some examples where the comparison of the intensity of the transient absorbance was important, the solutions were optically matched A_{266} = 0.37. The solutions were not purged with N_2 or O_2 prior to measurements. For each solution transient absorption spectra were recorded and decays of transient absorbance collected at 400, 410 and 420 nm. For the collection of decays at long time scales, a modification of the setup was used, wherein the probing light beam from the Xe-lamp was not pulsed, as previously described.[10] Intensity of the transient absorbance at these wavelengths immediately after the laser pulse and lifetime are compiled in Table S13. Spectra and decays are shown in the figures that follow.

The concentration of **1** in all samples for LFP was $c = 6.35 \times 10^{-4}$ M, concentration of sodium phosphate buffer was 0.1 M, CB[6] was 3.50×10^{-4} M or 1.40×10^{-3} M, and CB[7] was 6.79×10^{-4} M. The concentration of **2** in all samples for LFP was $c = 7.59 \times 10^{-4}$ M, concentration of sodium phosphate buffer was 0.092 M, CB[6] was 1.40×10^{-3} M, and CB[7] was 6.79×10^{-4} M. The real concentrations of the CB[n]s used in the experiment were determined by titration.[1]

Table S11. Data obtained by LFP of **1** in the presence of CB[6] and CB[7].

pH	4.41		7.00		9.08		10.77	
	Int.[a]	τ / ms	Int.	τ / ms	Int.	τ / ms	Int.	τ / ms
1	0.031	15±1	0.027	11±1	0.015	5.6±0.3	0.021	2.0±0.5
	0.025		0.028		0.021		0.020	
	0.027		0.025		0.015		0.020	
1@CB[6][b]	0.029	14±1	0.031	12±1	0.021	4.0±0.5	0.019	2.0±0.2
	0.028		0.021		0.018		0.019	
	0.024		0.023		0.018		0.019	
1@CB[6][c]	0.028	8.9±0.3	0.026	11.5±0.5	0.030	6±1	0.020	1.4±0.4
	0.027		0.026		0.031		0.019	
	0.026		0.026		0.025		0.020	
1@CB[7]	0.024	12.3±0.5	0.020	11±1	0.030	6.5±0.5	0.020	1.5±0.1
	0.024		0.024		0.028		0.018	
	0.022		0.026		0.028		0.015	

[a] Intensity of the transient absorbance at 400, 410 and 420 nm immediately after the laser pulse. [b] c(CB[6]) = 3.50 ×10^{-4} M. [c] c(CB[6]) = 1.40 ×10^{-3} M.

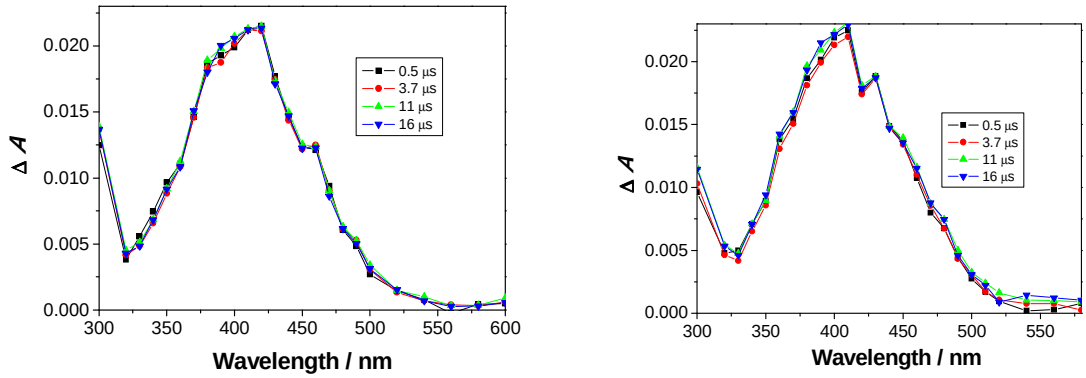

Fig S23. Transient absorption spectra of $\mathbf{1}^+$ (c = 6.35 × 10^{-4} M) in CH_3CN-H_2O (1:9) at pH 4.41 without CB (left) and in the presence of CB[6] c= 3.50 × 10^{-4} M (right).

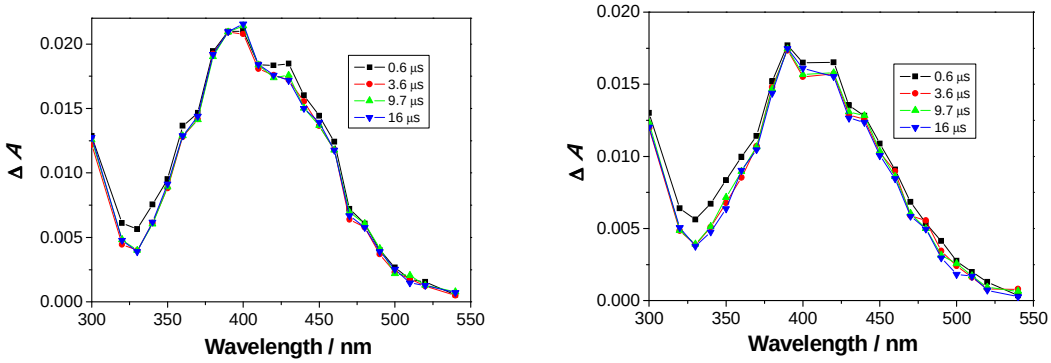

Fig S24. Transient absorption spectra of $\mathbf{1}^+$ (c = 6.35 × 10^{-4} M) in CH_3CN-H_2O (1:9) at pH 4.41 in the presence of CB[6] c = 1.40 × 10^{-3} M (left), and CB[7] c = 6.79 × 10^{-4} M (right).

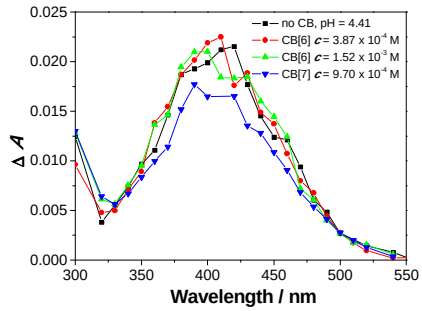

Fig S25. Transient absorption spectra of $\mathbf{1}^+$ (c = 6.35 × 10^{-4} M) in CH_3CN-H_2O (1:9) at pH 4.41 at delay of 0.5 µs without CB and in the presence of CB[6] c = 3.50 × 10^{-4}, CB[6] c = 1.40 × 10^{-3} M and CB[7] c = 6.79 × 10^{-4} M. The solutions were optically matched A_{266} = 0.37. The solutions were optically matched A_{266} = 0.37 and were not purged with N_2 or O_2 prior to measurements.

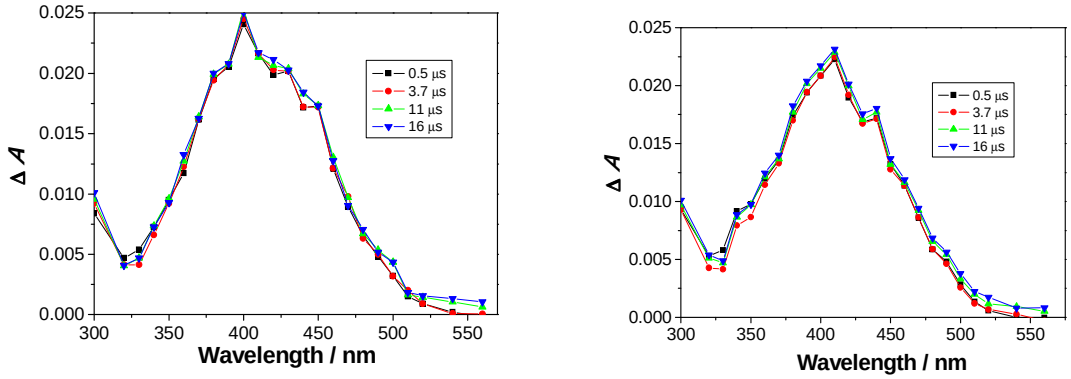

Fig S26. Transient absorption spectra of $\mathbf{1}^+$ (c = 6.35 × 10^{-4} M) in CH_3CN-H_2O (1:9) at pH 7.00 without CB (left) and in the presence of CB[6] c = 3.50 × 10^{-4} M (right).

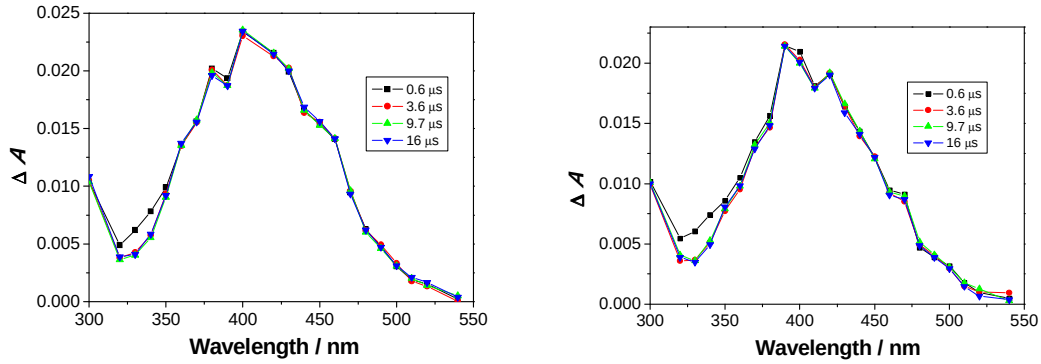

Fig S27. Transient absorption spectra of $\mathbf{1}^+$ (c = 6.35 × 10^{-4} M) in CH_3CN-H_2O (1:9) at pH 7.00 in the presence of CB[6] c= 1.40 × 10^{-3} M (left), and CB[7] c = 6.79 × 10^{-4} M (right).

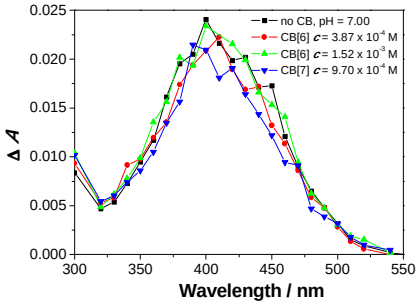

Fig S28. Transient absorption spectra of $\mathbf{1}^+$ (c = 6.35 × 10^{-4} M) in CH_3CN-H_2O (1:9) at pH 7.00 without CB and in the presence of CB[6] c = 3.50 × 10^{-4}, CB[6] c = 1.40 × 10^{-3} M and CB[7] c = 6.79 × 10^{-4} M. The solutions were not optically matched (A_{266} = 0.37 for the solution without CB and with CB[6], whereas for the CB[7] solution A_{266} = 0.43).

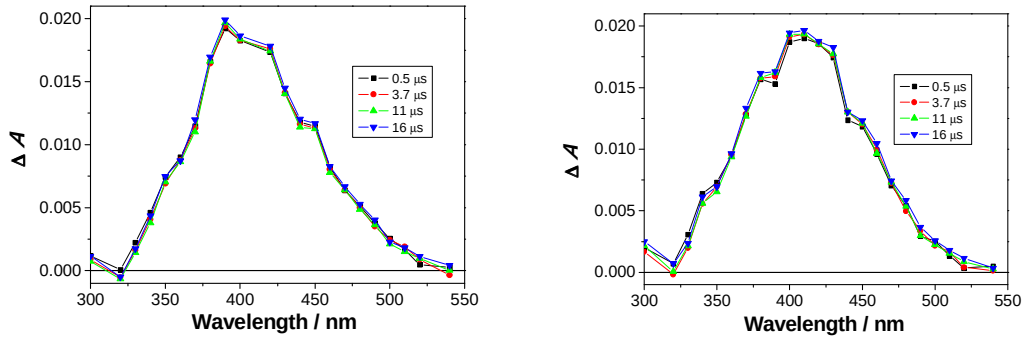

Fig S29. Transient absorption spectra of **1zw** (c = 6.35 × 10^{-4} M) in CH_3CN-H_2O (1:9) at pH 9.08 without CB (left) and in the presence of CB[6] c= 3.50 × 10^{-4} M (right).

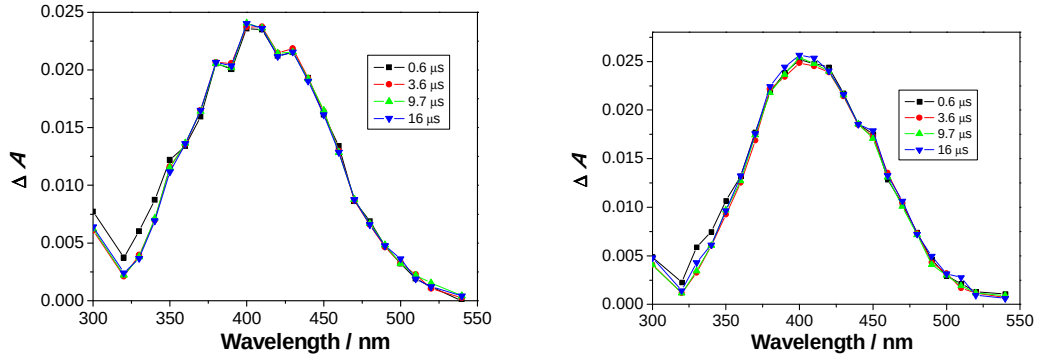

Fig S30. Transient absorption spectra of **1zw** (c = 6.35 × 10^{-4} M) in CH_3CN-H_2O (1:9) at pH 9.08 in the presence of CB[6] c= 1.40 × 10^{-3} M (left), and CB[7] c = 6.79 × 10^{-4} M (right).

Discussion of the LFP results

Transient absorption spectra of **1** in CH_3CN-H_2O were recorded for the aqueous solutions at different pH values. In all cases, a transient was detected absorbing with a maximum at 400-420 nm that decayed to the baseline with unimolecular kinetics. Based on literature precedent, the transient was assigned to **QM1**.[2]

Formation of the transient could not be resolved, it was formed within the laser pulse in all solutions at all pH values with or without CB[n].

The lifetime of the QM depends on pH, becoming shorter-lived in basic solution (Table S11). The finding is in accord with literature precedent. The intensity of the transient immediately after

the laser pulse allows for the comparison of the QM formation efficiency. However, at higher pH values (9 and 10), the absorbance of the solutions for the LFP measurements (**1zw** in the S_0) was lower than for the acidic and neutral solutions. Therefore, at pH > 9 no conclusion can be reached with respect to the influence of pH on the magnitude of the transient absorbance value. Nevertheless, irradiations of **1zw** at different pH values indicated that methanolysis (and formation of QMs) is more efficient at pH values where the molecule is in the zwitterionic form.[2]

At pH 4 and pH 7 all solutions were optically matched, allowing for the comparison of the efficiency of QM formation. Data in table S13 indicate that the addition of CB[6] did not affect the efficiency of the QM formation, whereas in the presence of CB[7] the efficiency was ≈15-20% lower. Very important finding is that QMs were formed in the presence of CB[n]s, although the phenol moiety is less acidic in the inclusion complex.

The lifetimes of QMs without CB[n] and in the presence of CB[n] are very similar, within experimental error. The only significant difference was observed for QM in the presence of CB[6] at pH 4.41. The finding is tentatively assigned to acid-catalyzed hydration of QM in the presence of CB[6] which is acidic due to inclusion of formic acid. Namely, formic acid was used in the purification of CB[6] sample.[11]

Similar lifetimes of QM in the presence of CB[n] can be due to the dissociation of the QM, formed inside of the CB[n] cavity. Therefore, QM has the same lifetime as when this transient is formed in the bulk of the solution. The other plausible explanation may be that QMs in the cavity of CB[n] are not protected from the attack by H_2O.

Inspection of the transient absorption spectra in the absence and presence of CB[6] and CB[7] indicate that all spectra look very similar. However, for the acidic and neutral solutions (pH 4-9) in the presence of CB[6] and CB[7] at short time scales (0.6-3.6 μs) a fast decay was observed at 330-380 nm. Such a decay was not observed for the solution not containing CB[n]. It is also important to note that the transient absorption spectrum at delay of 0.5 μs of an optically matched solution containing no CB[n] in this wavelength region has lower intensity then the spectra for solutions containing CB[6] or CB[7]. Consequently, this fast decay component with the rate constant of $k_{obs} \approx 1.1 \times 10^6$ s^{-1} is assigned to the dissociation of the QM from CB[n].

Table S12. Lifetimes of QM (ms) measured by LFP of **2** in the presence of CB[6] and CB[7].[a]

pH	**2**	**2@CB[6]**	**2@CB[7]**
3.00	1.6±0.3	-	2.0±0.3
	10-15		8-10
4.41	7±1	3±1	5.7±0.3
	30-50	20-40	30-35
6.00	4.4±0.3	5±1	4±1
	20-40	30-40	10-30 (hardly detectable)
7.00	2.0±0.2	3.0±0.3	2.0±0.5
8.00	2.0±0.5	2.0±0.4	2.0±0.5
10.41	1.8±0.2	1.7±0.2	1.3±0.2
12.31	0.60±0.05	-	0.6±0.1

[a] QM lifetimes at pH values < 7.0 are bi-exponential due to the reaction of QM giving adducts or new QM species. For details see ref. 2.

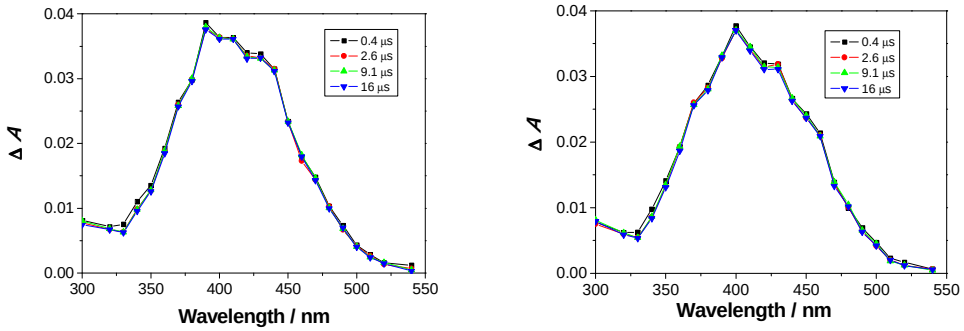

Fig S31. Transient absorption spectra of $\mathbf{2}^{2+}$ (c = 7.59 × 10^{-4} M) in CH_3CN-H_2O (1:9) at pH 3.00 (left) and in the presence of CB[7] c = 6.79 × 10^{-4} M (right).

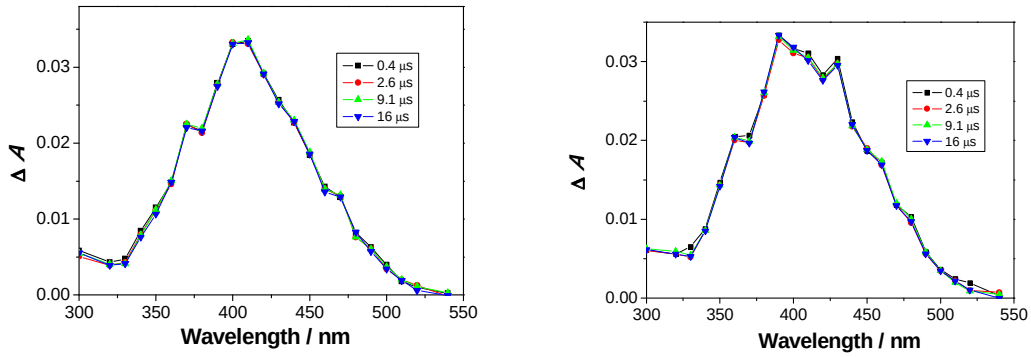

Fig S32. Transient absorption spectra of $\mathbf{2}^{2+}$ (c = 7.59 × 10^{-4} M) in CH_3CN-H_2O (1:9) at pH 4.41 (left) and in the presence of CB[7] c = 6.79 × 10^{-4} M (right).

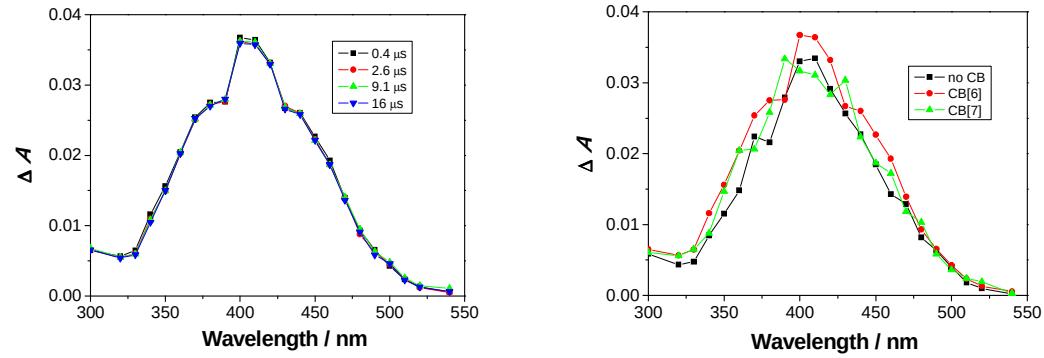

Fig S33. Transient absorption spectra of $\mathbf{2}^{2+}$ (c = 7.59 × 10^{-4} M) in CH_3CN-H_2O (1:9) at pH 4.41 and in the presence of CB[6] c = 1.40 × 10^{-3} M (left), and the spectra of $\mathbf{2}^{2+}$ at pH 4.41 without and in the presence of CB[6] c = 1.40 × 10^{-3} M and CB[7] c = 6.79 × 10^{-4} M at the delay of 0.4 µs (right), the absorbances were not optically matched.

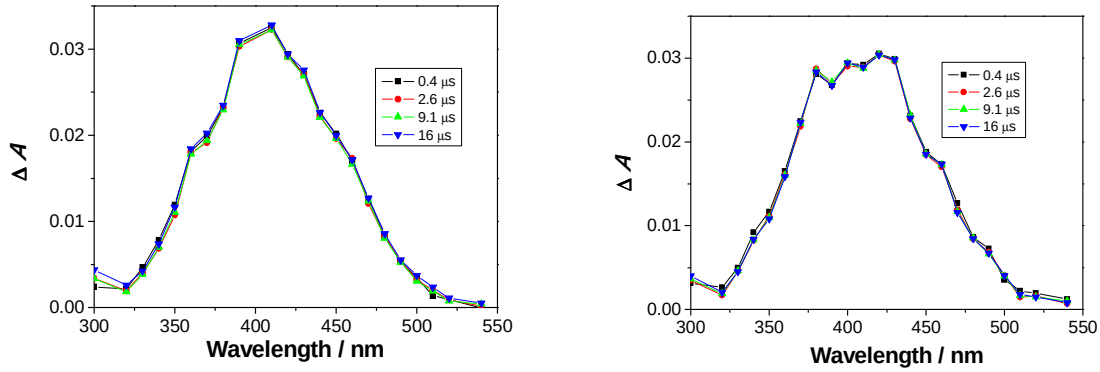

Fig S34. Transient absorption spectra of $\mathbf{2}^{+}$ (c = 7.59 × 10^{-4} M) in CH_3CN-H_2O (1:9) at pH 6.00 (left) and in the presence of CB[7] c = 6.79 × 10^{-4} M (right).

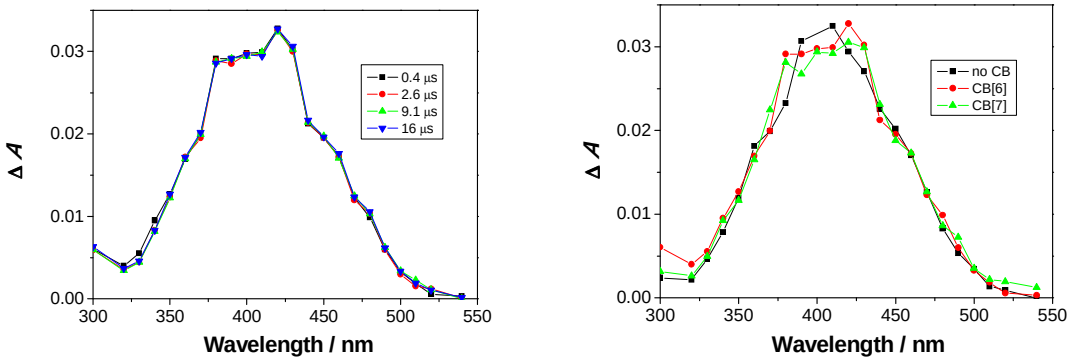

Fig S35. Transient absorption spectra of $\mathbf{2}^{+}$ (c = 7.59 × 10^{-4} M) in CH_3CN-H_2O (1:9) at pH 6.00 and in the presence of CB[6] c = 1.40 × 10^{-3} M (left), and the spectra of $\mathbf{2}^{+}$ at pH 6.00 without and in the presence of CB[6] c = 1.40 × 10^{-3} M and CB[7] c = 6.79 × 10^{-4} M at the delay of 0.4 µs (right), the absorbances were not optically matched.

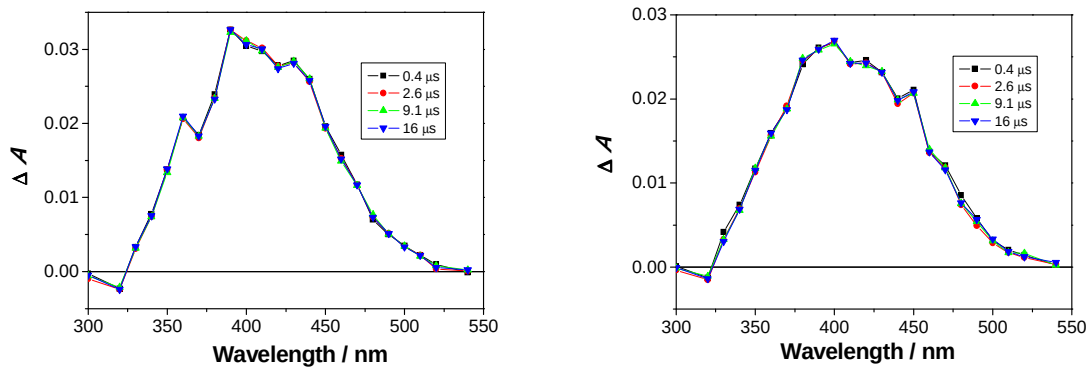

Fig S36. Transient absorption spectra of $\mathbf{2}^+$ (c = 7.59 × 10^{-4} M) in CH_3CN-H_2O (1:9) at pH 7.00 (left) and in the presence of CB[7] c = 6.79 × 10^{-4} M (right).

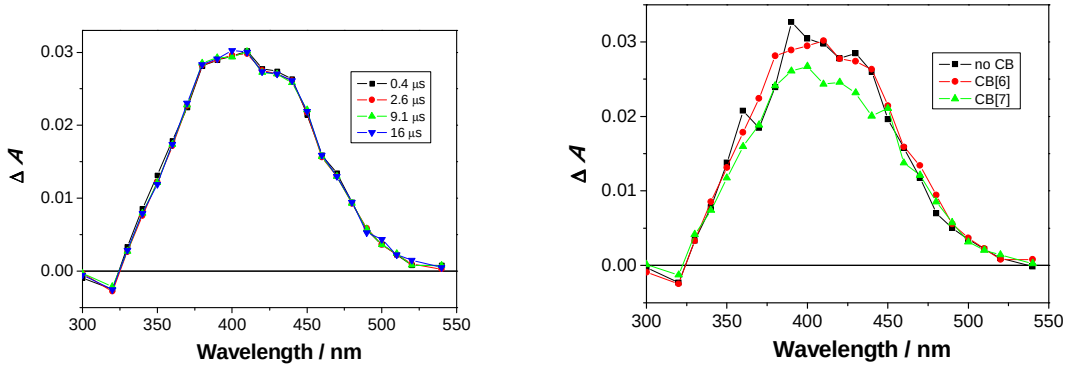

Fig S37. Transient absorption spectra of $\mathbf{2}^+$ (c = 7.59 × 10^{-4} M) in CH_3CN-H_2O (1:9) at pH 7.00 and in the presence of CB[6] c = 1.40 × 10^{-3} M (left), and the spectra of $\mathbf{2}^+$ at pH 7.00 without and in the presence of CB[6] c = 1.40 × 10^{-3} M and CB[7] c = 6.79 × 10^{-4} M at the delay of 0.4 µs (right), the absorbances for the solution without CB and with CB[6] were optically matched (A_{266} = 0.28) and for the CB[7] was higher (A_{266} = 0.35).

Discussion of the LFP results

The main finding from the LFP measurements is that QM can be formed from **2** when it is complexed with CB[6] and CB[7]. Formation of QM was observed at all pH values and the data suggests that efficiency of the QM formation is increased in the presence of CB[6] and decreased in the presence of CB[7].

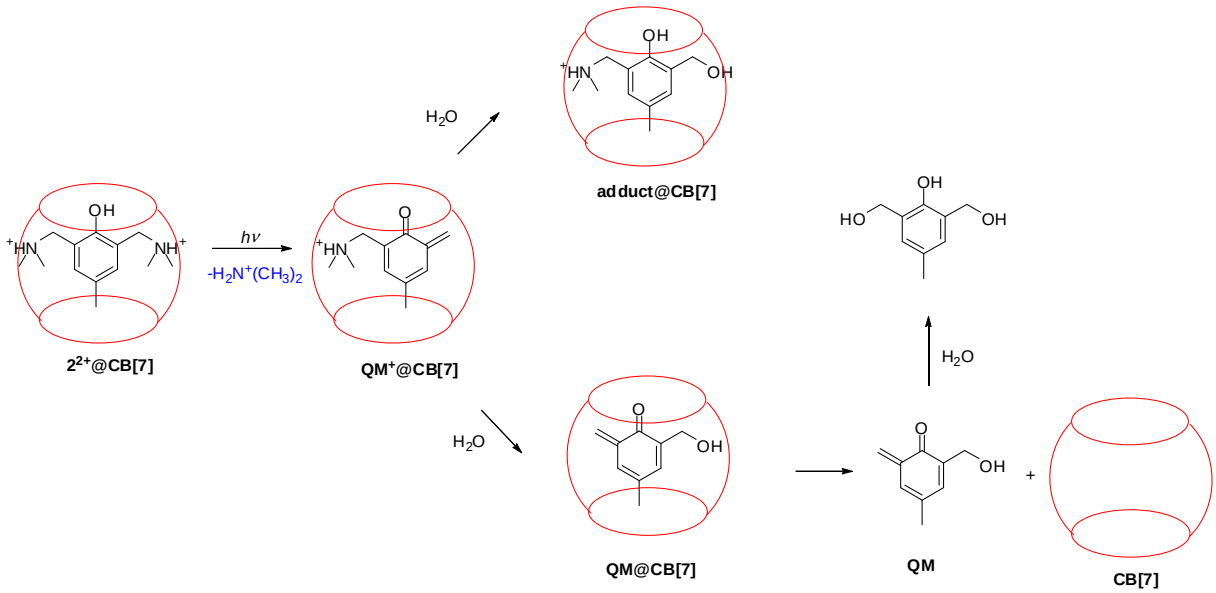

Scheme S3.

Lifetimes of QM depend on pH. At pH<7, a bi-exponential decay was observed that was assigned to the reaction giving H_2O-adduct, or new QM species.[2] At pH>7 decay of QM follows unimolecular kinetics. No effect of CB[n] on the lifetime of the QM was observed. It would be interesting to compare the contribution of the decay components with and without CB[n]. However, any quantitative analysis is difficult due to the poor quality of the decays collected at long time scale. It seems that at pH 4 CB[6] and CB[7] increase contribution of the long-lived component, but at pH 6 the trend is opposite.

It should be mentioned that the fast decay of the transient absorption at 330-350 nm in the presence of CB[6] and CB[7] was not observed. The decay observed for $\mathbf{1}^+$ was assigned to the exit kinetics of QM from CB[n]. The QM formed from $\mathbf{2}^{2+}$ should be charged, so it is anticipated that the exit should be slower. In conclusion, our results suggest that QM formed from $\mathbf{1}^+$ exits CB, whereas QM from $\mathbf{2}^{2+}$ has probably slow exit kinetics that cannot be observed by LFP.

8. Antiproliferative tests

Compounds

Table S13. Samples used in the biological testing and concentrations of hosts and/or guests used in the samples. The solutions were prepared in 0.3% NaCl.

Compound/Tested solution I.D.	*c*(Compound)/ M	*c*(CB[n])/M
1	1×10^{-2}	-
2	1×10^{-2}	-
CB[6]	-	1×10^{-2}
CB[7]	-	1×10^{-2}
1+CB[6]	1×10^{-2}	1×10^{-2}
2+CB[6]	1×10^{-2}	1×10^{-2}
1+CB[7]	1×10^{-2}	1×10^{-2}
2+CB[7]	1×10^{-2}	1×10^{-2}

Cell lines

The experiments were carried out on 2 human cell lines which are derived from 2 cancer types. The following cell lines were used: H460 (lung carcinoma) and MCF-7 (breast carcinoma).

Cell culturing

H460 and MCF-7 cells were cultured as monolayers and maintained in Dulbecco's modified Eagle medium (DMEM), supplemented with 10% fetal bovine serum (FBS), 2 mM L-glutamine, 100 U/mL penicillin and 100 μg/mL streptomycin in a humidified atmosphere with 5% CO_2 at 37 °C.

Proliferation assays

The panel cell lines were inoculated in parallel onto a series of standard 96-well microtiter plates on day 0, at 1×10^4 to 3×10^4 cells/mL, depending on the doubling times of specific cell line.

Test agents were then added in five 10-fold dilutions (10^{-8} to 10^{-4} M) and incubated for further 72 h. Working dilutions were freshly prepared on the day of testing.

For each cell line one of the plates was left in the dark, while the other was irradiated in a Luzchem reactor (6 lamps 300 nm, 1 min) 4 h after the addition of the compounds and subsequently 24 h and 48 h after first irradiation, as described above. The solvent was also tested for eventual inhibitory activity by adjusting its concentration to be the same as in working concentrations. After 72 h of incubation the cell growth rate was evaluated by performing the MTT assay, which detects dehydrogenase activity in viable cells. The MTT Cell Proliferation Assay is a colorimetric assay system, which measures the reduction of a tetrazolium component (MTT) into an insoluble formazan product by the mitochondria of viable cells.[12] For this purpose the substance treated medium was discarded and MTT was added to each well at a concentration of 20 μg/40 μL. After 4 h of incubation the precipitates were dissolved in 160 μL of dymethyl-sulfoxide (DMSO). The absorbance (*A*) was measured on a microplate reader at 570 nm. The absorbance is directly proportional to the cell viability. The percentage of growth (PG) of the cell lines was calculated according to one or the other of the following two expressions:

If (mean A_{test} – mean A_{tzero}) ≥ 0 then

$$PG = 100 \times (\text{mean } A_{test} - \text{mean } A_{tzero}) / (\text{mean } A_{ctrl} - \text{mean } A_{tzero}).$$

If (mean A_{test} – mean A_{tzero}) < 0 then:

$$PG = 100 \times (\text{mean } A_{test} - \text{mean } A_{tzero}) / A_{tzero}.$$

Where:

Mean A_{tzero} = the average of absorbance measurements before exposure of cells to the test compound.

Mean A_{test} = the average of absorbance measurements after the desired period of time.

Mean A_{ctrl} = the average of absorbance measurements after the desired period of time with no exposure of cells to the test compound.

Each test point was performed in quadruplicate. The results were expressed as GI_{50}, a concentration necessary for 50% of inhibition. Each result is a mean value from at least two separate experiments.

GI_{50}

The GI_{50} measures the growth inhibitory power of the test agent and represents the concentration that causes 50% growth inhibition. The GI_{50} values for each compound are calculated from dose-response curves using linear regression analysis by fitting the test concentrations that give PG values above and below the respective reference value (e.g. 50 for GI_{50}). Therefore, a "real" value for any of the response parameters is obtained only if at least one of the tested drug concentrations falls above, and likewise at least one falls below the respective reference value. However, if for a given cell line all of the tested concentrations produce PGs exceeding the respective reference level of effect (e.g. PG value of 50), then the highest tested concentration is assigned as the default value.

Table S14. GI_{50} values (in μM)[a]

Compound/ Tested solution	Cell lines			
	MCF-7		H 460	
	Not irradiated	Irradiated 300nm 3×1 min	Not irradiated	Irradiated 300nm 3×1 min
1	≥100	≥100	≥100	≥100
2	23±5	≥100	32±4	≥100
CB[6]	≥100	≥100	≥100	≥100
CB[7]	≥100	≥100	≥100	≥100
1+CB[6]	≥100	≥100	≥100	≥100
2+CB[6]	50±40	≥100	31±2	≥100
1+CB[7]	≥100	38±19	≥100	≥100
2+CB[7]	28±5	≥100	18±7	≥100

[a] GI_{50}; the concentration that causes 50% growth inhibition

Discussion of antiproliferative results

Antiproliferative tests with **1** and **2** were performed in the presence of cucurbit[n]urils on two human cancer cell lines H460 (lung carcinoma) and MCF-7 (breast carcinoma) to establish the potential biological application of this supramolecular delivery system. MTT tests were performed on cells treated with compounds **1** and **2**, CB[6], CB[7], or their mixtures where the cells were kept either in the dark, or irradiated for 3×1 min at 300 nm (for details see Tables above). CB[n], compound **1**, **1+CB[6]** and **1+CB[7]** in isolation exhibit no cytotoxicity at any of the concentrations tested. However, **2** and the mixtures **2+CB[6]** and **2+CB[7]** show weak antiproliferative effects at micromolar concentrations in the dark. Upon irradiation of cancer cells, the antiproliferative effect of **1+CB[7]** is enhanced, which would be in line with the hypothesis of the formation of QM in the inclusion complex (**1@CB[7]**) inside the cells. On the contrary, antiproliferative activity of **2, 2+CB[6]** and **2+CB[7]** was diminished upon irradiation of cancer cells, which would indicate the formation of inactive compounds, such as the product of the photohydrolysis of the active compound.

9. Molecular modeling

Coordinates

1^{+}-*syn*

Atom number	Atom type	x	y	z
1	N	-2.8310	1.8646	-0.0005
2	C	-2.2245	2.4593	1.2504
3	C	-2.0471	2.2475	-1.2354
4	C	-6.1088	-3.5718	0.2292
5	C	-6.8704	0.1415	-0.1387
6	C	-7.0565	-1.2359	-0.0354
7	C	-5.9523	-2.0766	0.1137
8	C	-4.6842	-1.4905	0.1536
9	C	-4.4752	-0.1071	0.0512
10	C	-5.5988	0.7237	-0.0983
11	O	-5.5044	2.0709	-0.2056
12	C	-3.0280	0.3620	0.1135
13	H	-3.7525	2.3299	-0.1060
14	H	-2.1684	3.5674	1.1598
15	H	-2.8644	2.2286	2.1321
16	H	-1.1991	2.0623	1.4278
17	H	-1.9910	3.3556	-1.3255
18	H	-2.5594	1.8644	-2.1469
19	H	-1.0120	1.8387	-1.1973
20	H	-7.1741	-3.8898	0.1812
21	H	-5.5657	-4.0810	-0.5992
22	H	-5.6921	-3.9289	1.1984
23	H	-7.7537	0.7912	-0.2560
24	H	-8.0756	-1.6527	-0.0720

25	H	-3.8115	-2.1542	0.2712
26	H	-6.3770	2.4824	-0.3016
27	H	-2.5928	-0.0074	1.0712
28	H	-2.4681	-0.1579	-0.6985

1^{+}-*anti*

Atom number	Atom type	x	y	z
1	N	-1.3078	-0.4536	0.1619
2	C	-0.0249	-0.0636	0.8378
3	C	-1.4361	0.1865	-1.1928
4	C	-5.6447	-4.1516	0.7054
5	C	-5.8896	-0.5842	-0.6502
6	C	-6.1803	-1.9124	-0.3578
7	C	-5.3010	-2.7171	0.3867
8	C	-4.1163	-2.1291	0.8297
9	C	-3.7900	-0.7928	0.5426
10	C	-4.6929	-0.0167	-0.2042
11	O	-4.3371	1.2770	-0.4701
12	C	-2.5282	-0.1864	1.0716
13	H	-1.2916	-1.4675	0.0126
14	H	-0.0464	1.0106	1.0243
15	H	0.0604	-0.6040	1.7807
16	H	0.8135	-0.3120	0.1867
17	H	-1.4916	1.2663	-1.0597
18	H	-2.3478	-0.1737	-1.6643
19	H	-0.5641	-0.0837	-1.7889
20	H	-6.5835	-4.2181	1.2650
21	H	-5.7715	-4.7419	-0.2084
22	H	-4.8654	-4.6277	1.3055

23	H	-6.5919	0.0144	-1.2248
24	H	-7.1175	-2.3333	-0.7108
25	H	-3.4328	-2.7174	1.4400
26	H	-5.0772	1.7479	-0.8778
27	H	-2.2547	-0.6150	2.0382
28	H	-2.5948	0.8990	1.1606

2^{2+}*-syn-syn trans*

Atom number	Atom type	x	y	z
1	C	-4.3555	-0.4015	-0.7753
2	C	-4.0263	-1.4642	0.0734
3	C	-2.7049	-1.7360	0.4542
4	C	-1.7028	-0.9133	-0.0709
5	C	-1.9851	0.1551	-0.9368
6	C	-3.3263	0.4228	-1.2547
7	O	-3.6994	1.4705	-2.0939
8	C	-0.8608	0.9826	-1.5039
9	C	-2.3756	-2.8914	1.3655
10	N	-0.5768	0.6752	-2.9826
11	C	-0.0924	-0.7365	-3.2011
12	C	0.3814	1.6766	-3.5795
13	C	-5.7812	-0.2072	-1.2343
14	N	-6.3603	1.1606	-0.8883
15	C	-7.6837	1.3832	-1.5743
16	C	-6.4637	1.3956	0.5943
17	H	-4.8222	-2.1030	0.4480
18	H	-0.6688	-1.1029	0.2063
19	H	-3.1758	2.2635	-1.9056
20	H	-1.0459	2.0608	-1.4623
21	H	0.0743	0.7964	-0.9723

22	H	-3.1947	-3.1003	2.0575
23	H	-2.1977	-3.8048	0.7855
24	H	-1.4759	-2.6943	1.9529
25	H	-1.4715	0.7695	-3.4756
26	H	-0.8150	-1.4314	-2.7768
27	H	0.0110	-0.9054	-4.2730
28	H	0.8759	-0.8474	-2.7112
29	H	1.3303	1.6096	-3.0461
30	H	0.5286	1.4380	-4.6329
31	H	-0.0363	2.6786	-3.4786
32	H	-5.8609	-0.2886	-2.3216
33	H	-6.4427	-0.9504	-0.7850
34	H	-5.6885	1.8329	-1.2775
35	H	-8.0434	2.3826	-1.3289
36	H	-7.5467	1.2881	-2.6516
37	H	-8.3923	0.6348	-1.2172
38	H	-6.7890	2.4220	0.7654
39	H	-5.4906	1.2255	1.0528
40	H	-7.1985	0.7014	1.0047

2^{2+}*-syn-syn cis*

Atom number	Atom type	x	y	z
1	C	-4.6523	-0.6029	-0.5093
2	C	-4.6402	-1.8364	0.1570
3	C	-3.4481	-2.4527	0.5563
4	C	-2.2451	-1.7877	0.2754
5	C	-2.2153	-0.5557	-0.3883
6	C	-3.4302	0.0243	-0.7793
7	O	-3.4262	1.3038	-1.3658
8	C	-0.8969	0.0818	-0.7547

9	C	-3.4464	-3.7952	1.2410
10	N	-0.6984	1.4675	-0.1409
11	C	-0.6057	1.4278	1.3600
12	C	0.4903	2.1702	-0.7442
13	C	-5.9523	-0.0199	-1.0084
14	N	-6.2665	1.3588	-0.4269
15	C	-7.4209	2.0078	-1.1465
16	C	-6.5003	1.3213	1.0582
17	H	-5.5841	-2.3359	0.3588
18	H	-1.3073	-2.2516	0.5710
19	H	-3.3603	1.2320	-2.3327
20	H	-0.0556	-0.5311	-0.4254
21	H	-0.8050	0.2257	-1.8351
22	H	-4.4335	-4.0506	1.6314
23	H	-3.1543	-4.5834	0.5373
24	H	-2.7330	-3.8196	2.0695
25	H	-1.5419	1.9954	-0.3984
26	H	-0.5714	2.4501	1.7379
27	H	-1.4744	0.9054	1.7584
28	H	0.3084	0.9008	1.6370
29	H	0.5765	3.1620	-0.2996
30	H	0.3480	2.2549	-1.8219
31	H	1.3868	1.5872	-0.5290
32	H	-5.9423	0.1161	-2.0937
33	H	-6.7973	-0.6646	-0.7588
34	H	-5.4241	1.9194	-0.6084
35	H	-7.5895	2.9974	-0.7210
36	H	-7.1803	2.0928	-2.2065
37	H	-8.3090	1.3889	-1.0117
38	H	-6.6127	2.3427	1.4228

39	H	-5.6529	0.8371	1.5417
40	H	-7.4141	0.7574	1.2515

2^{2+}*-syn-anti cis*

Atom number	Atom type	x	y	z
1	C	-4.3783	-1.0568	0.4228
2	C	-4.4613	-2.3833	-0.0051
3	C	-3.3204	-3.1905	-0.1464
4	C	-2.0823	-2.6115	0.1434
5	C	-1.9513	-1.2683	0.5356
6	C	-3.1142	-0.5011	0.6877
7	O	-3.0623	0.8506	1.0328
8	C	-0.5861	-0.7043	0.8466
9	C	-3.4430	-4.6331	-0.5659
10	N	0.3263	-0.6206	-0.3806
11	C	1.7563	-0.3436	0.0163
12	C	-0.1641	0.3708	-1.4014
13	C	-5.6350	-0.2659	0.7067
14	N	-5.7131	1.0551	-0.0490
15	C	-5.8241	0.8675	-1.5365
16	C	-6.8250	1.9246	0.4778
17	H	-5.4384	-2.8165	-0.2037
18	H	-1.1936	-3.2374	0.0792
19	H	-2.8517	0.9645	1.9727
20	H	-0.0563	-1.3366	1.5636
21	H	-0.6364	0.3100	1.2437
22	H	-4.0002	-5.2090	0.1804
23	H	-3.9830	-4.7241	-1.5136
24	H	-2.4652	-5.1033	-0.6875
25	H	0.3069	-1.5440	-0.8261

26	H	1.7959	0.6252	0.5153
27	H	2.0976	-1.1297	0.6901
28	H	2.3729	-0.3267	-0.8825
29	H	-0.1268	1.3671	-0.9596
30	H	-1.1854	0.1131	-1.6767
31	H	0.4856	0.3245	-2.2755
32	H	-6.5294	-0.8345	0.4447
33	H	-5.6994	-0.0016	1.7659
34	H	-4.8187	1.5218	0.1561
35	H	-5.7596	1.8424	-2.0199
36	H	-5.0151	0.2221	-1.8757
37	H	-6.7881	0.4073	-1.7577
38	H	-6.8256	2.8665	-0.0710
39	H	-6.6600	2.1111	1.5391
40	H	-7.7740	1.4074	0.3306

2^{2+}*-anti-anti trans*

Atom number	Atom type	x	y	z
1	C	-4.6816	-2.0588	0.7504
2	C	-4.7831	-3.4522	0.8406
3	C	-3.6566	-4.2750	0.9044
4	C	-2.4001	-3.6678	0.8796
5	C	-2.2612	-2.2809	0.7744
6	C	-3.4059	-1.4672	0.7016
7	O	-3.2516	-0.1244	0.5541
8	C	-0.8627	-1.6875	0.7725
9	C	-3.7746	-5.7748	1.0050
10	N	-0.0998	-2.0637	-0.4831
11	C	1.3559	-1.6664	-0.3913
12	C	-0.7467	-1.5133	-1.7335

13	C	-5.9656	-1.2459	0.7057
14	N	-6.9385	-1.6605	1.8005
15	C	-8.2956	-1.0224	1.6106
16	C	-6.3879	-1.3887	3.1822
17	H	-5.7809	-3.9182	0.8591
18	H	-1.4990	-4.2991	0.9394
19	H	-4.0792	0.3173	0.3116
20	H	-0.3313	-2.0969	1.6635
21	H	-0.8692	-0.5819	0.8955
22	H	-4.8332	-6.1168	1.0262
23	H	-3.2800	-6.2579	0.1319
24	H	-3.2831	-6.1377	1.9362
25	H	-0.1268	-3.1076	-0.5570
26	H	1.4640	-0.5611	-0.3094
27	H	1.8308	-2.1412	0.4964
28	H	1.9081	-2.0157	-1.2925
29	H	-0.7678	-0.4002	-1.7156
30	H	-1.7884	-1.8908	-1.8346
31	H	-0.1861	-1.8477	-2.6351
32	H	-6.4277	-1.4315	-0.2921
33	H	-5.7725	-0.1532	0.7850
34	H	-7.0768	-2.6946	1.7208
35	H	-8.2294	0.0869	1.6812
36	H	-8.7145	-1.2957	0.6161
37	H	-9.0056	-1.3901	2.3851
38	H	-6.2164	-0.2994	3.3368
39	H	-5.4261	-1.9270	3.3350
40	H	-7.0984	-1.7537	3.9574

10. References

[1] Yi, S.; Kaifer, A. E., *J. Org. Chem*. **2011**, *76*, 10275-10278.

[2] Škalamera, Đ.; Bohne, C.; Landgraf, S.; Basarić, N., *J. Org. Chem*. **2015**, *80*, 10817-10828.

[3] Mohanty, J.; Bhasikuttan, A.C.; Nau, W.M.; Pal, H., *J. Phys. Chem. B* **2006**, *110*, 5132-5138; Koner, A.L.; Ghosh, I.; Saleh, N.; Nau, W.M., *Can. J. Chem*. **2011**, *89*, 139-147; Shaikh, M.; Dutta Choudhury, S.; Mothany, J.; Bhasikuttan, A.C.; Nau, W.M.; Pal, H., *Chem. Eur. J*. **2009**, *15*, 12362-12370.

[4] Glasoe, P. K.; Long, F. A., *J. Phys. Chem.* **1960**, *64*, 188-189.

[5]. Lagona, J.; Mukhopadhyay, P.; Chakrabarti, S.; Isaacs, L., *Angew. Chem. Int. Ed.* **2005**, *44*, 4844–4870.

[6] Frisch, M.J. et al. Gaussian 09, Revision D.01, Gaussian, Inc., Wallingford CT, 2013.

[7]. Kim, K.; Kim, H.-J., Cucurbituril, Its Homologues, and Derivatives, *in Enyclopedia of Supramolecular Chemistry*, Atwood, J. R.; Steed, J. W. (Editors), vol. 1, Taylor & Francis, 2004., Boca Raton, US, pp. 390.

[8] (a) Program for fitting available at: www.chem.unsw.edu.au/research/groups/thordarson/fittingprogram; (b) Thordarson, P. *Chem. Soc. Rev.* **2011**, *40*, 1305-1323.

[9] Silverstein, R. M.; Webster, F. X., Spectrometric Identification of Organic Compounds, 6th ed. John Wiley, New York, 1998.

[10] Liao, Y.; Bohne, C. *J. Phys. Chem.* **1996**, *100*, 734-743.

[11] Huang, W. H.; Liu, S.; Isaacs, L., In Modern Supramolecular Chemistry: Strategies for Macrocycle Synthesis, Eds. Diederich, F.; Stang, P. J.; Tykwinski, R. R., WILEY-VCH, Weinheim 2008.

[12] Mossman, T., *J Immunol Meth* **1983**, *65*, 55-63; (b) Boyd, M.R.; Kenneth, DP., *Drug Dev Res* **1995**, 34:91-109; (c) www.dtp.nci.nih.gov